Self-force and fluid resonances

Soichiro Isoyama and Raissa F. P. Mendes
Department of Physics, University of Guelph, Guelph, Ontario, N1G 2W1, Canada

Eric Poisson
Department of Physics, University of Guelph, Guelph, Ontario, N1G 2W1, Canada and
Canadian Institute for Theoretical Astrophysics, University of Toronto, Toronto, Ontario, M5S 3H8, Canada

(Dated: December 2, 2015)

The gravitational self-force acting on a particle orbiting a massive central body has thus far been computed for vacuum spacetimes involving a black hole. In this work we continue an ongoing effort to study the self-force in nonvacuum situations. We replace the black hole by a material body consisting of a perfect fluid, and determine the impact of the fluid's dynamics on the self-force and resulting orbital evolution. We show that as the particle inspirals toward the fluid body, its gravitational perturbations trigger a number of quasinormal modes of the fluid-gravity system, which produce resonant features in the conservative and dissipative components of the self-force. As a proof-of-principle, we demonstrate this phenomenon in a simplified framework in which gravity is mediated by a scalar potential satisfying a wave equation in Minkowski spacetime.

arXiv:1512.00059v1 [gr-qc] 30 Nov 2015

I. INTRODUCTION AND SUMMARY

The inspiral of a solar-mass compact object into a supermassive black hole is a promising source of low-frequency gravitational waves for space-based detectors such as eLISA [1] and DECIGO [2]. This observation has motivated a sustained effort to model the orbital motion of such a system, in a treatment that goes beyond the test-mass approximation in which the compact object moves on a geodesic in the background spacetime of the large black hole. In this improved treatment [3, 4], the gravitational influence of the small body is taken into account, and the motion is geodesic in the perturbed spacetime instead of the background spacetime. Alternatively, the motion of the small body can still be viewed in the background spacetime, where it is now accelerated, the acceleration being caused by the gravitational perturbation created by the body. In this view, the body experiences a gravitational self-force, and it is this self-force that is responsible for the inspiraling motion.

To date the gravitational self-force was formulated rigorously [5–7], it was computed and implemented in orbital evolutions around nonrotating black holes [8, 9], it was implicated in an improved calculation of the innermost circular orbit of a Kerr black hole [10], and its role was elucidated in attempts to violate cosmic censorship by overspinning a near-extremal black hole [11–14]. The gravitational self-force was extended to second order in perturbation theory [15–19], and its consequences were compared to the predictions of high-order post-Newtonian theory [20–22] and numerical relativity [23]. Other achievements of the gravitational self-force program are reviewed in Refs. [24, 25].

Until recently the gravitational self-force was formulated and computed for bodies moving in vacuum spacetimes, for which the background metric satisfies the Einstein field equations in the absence of a matter term. This restriction, of course, is amply justified for the applications reviewed previously, in which the large body is a black hole. Other applications, however, may well involve the presence of matter. An example of such a situation is the recent effort [26] to take into account self-force effects in attempts to overcharge a near-extremal black hole [27] (this is the charged version of the overspinning scenario described previously). In this situation the black hole is charged, the spacetime is filled with an electrostatic field, and the coupling between gravitational and electromagnetic perturbations creates complications in the formulation of the self-force. In this case an adequate formulation of the self-force for background spacetimes containing either a scalar or electromagnetic field was provided by Zimmerman and Poisson [28, 29] and Linz, Friedman, and Wiseman [30]. In a related development, the self-force was extended to scalar-tensor theories of gravity by Zimmerman [31].

The presence of a scalar or electromagnetic field in the background spacetime makes a concrete and convenient starting point for the formulation of the self-force in nonvacuum situations, but other applications call for the presence of other types of matter fields. The example that motivates the work presented in this paper is the self-forced motion of a small object around a large material body made up of a perfect fluid. There is currently no formulation of the self-force that accounts for the coupling between the gravitational and fluid perturbations that arise in such systems. A self-force formulation that achieves this would have some use. For example, one could use this self-force to test the hypothesis that the central body is a black hole by comparing its predictions to those of an alternative hypothesis, in which the central body is a fluid body in hydrostatic equilibrium.

Our goal in this paper is not to provide such a general formulation of the self-force. What we wish to do instead is to explore the expected physical consequences of the gravity-matter coupling on the self-force. This coupling gives rise

to a discrete spectrum of quasinormal modes, and we wish to explore the impact of these modes on the gravitational self-force. What intrigues us the most is the possibility that resonances can occur when the orbital frequency is in a commensurate relation with a quasinormal-mode frequency; we wish to determine the role of these resonances on the inspiraling motion of the particle. The purely dissipative aspects of this problem are already understood, and can be inferred from the impact of the resonances on the radiative fluxes of energy and angular momentum from the system [32–34]. But we wish here to consider all aspects of the self-force, both conservative and dissipative. Our analysis is a rudimentary one that serves as a proof-of-principle. We believe that our results motivate a deeper investigation, which we leave for future work.

In this spirit of proof-of-principle, we choose to avoid the technical complications associated with a perturbed fluid system in general relativity. For this exploration we consider a much simpler theory of gravity implicating a flat spacetime with Minkowski metric $\eta_{\alpha\beta}$ and a scalar gravitational potential Φ. (In this paper, we adopt geometric units, setting $G = c = 1$, and metric signature +2. Latin and Greek indices run from 1 to 3, and from 0 to 3, respectively.) The fluid is described by its energy-momentum tensor $T^{\alpha\beta}$. The gravitational field equation is chosen to be

$$\Box\Phi = 4\pi T^{\mu}_{\ \mu}, \tag{1.1}$$

and the fluid equations are

$$\nabla_\beta T^{\alpha\beta} = -T^{\mu}_{\ \mu}\nabla^\alpha\Phi, \tag{1.2}$$

where ∇_α is the covariant-derivative operator compatible with the Minkowski metric. This special-relativistic theory is obviously incompatible with observational tests, and we certainly do not claim that it is a viable description of gravity. It is not. We find, nevertheless, that it provides a useful and simple framework to explore the impact of the fluid-gravity coupling on the self-force. One important feature of the theory is that it automatically incorporates a source of dissipation: the gravitational potential satisfies a wave equation, and the gravitational waves carry energy away from the system. This radiative loss permits the inspiral of a particle moving around a fluid body. The full set of equations associated with the scalar theory is presented in Sec. III.

In Sec. IV we construct stellar models in the scalar theory of gravity. We consider a static and spherically symmetric distribution of perfect fluid, and choose the equation of state to be a slight modification of $p \propto \rho^2$, where p is the pressure and ρ the rest-mass density; the modified (but still physical) equation of state allows us to find simple analytical solutions to the structure equations. Our unperturbed body has a mass M and radius R.

In Sec. V we perturb the stellar model and derive the coupled equations that govern the fluid and gravitational perturbations. In the absence of an external forcing term, the equations are homogeneous and represent an eigenvalue system for the quasinormal modes. We integrate these equations, and obtain a number of modes, those displayed in Fig. 1. The spectrum delivered by the scalar theory is fairly typical, but we notice the presence of some unstable modes (indicated with circles in the figure). We also see that the mode lifetime (measured by $|\mathrm{Im}(\omega)|^{-1}$) can be extremely long for some modes, and this shall have an impact on the width of the resonances identified below.

In Sec. VI we place a particle of mass $\mathfrak{m}$ on a circular orbit of radius r_0 and angular frequency Ω around the fluid star, and reformulate the perturbation equations to account for the presence of the particle. The force exerted on the particle by the star is $f_\alpha = \mathfrak{m}(\delta_\alpha^{\ \beta} + v_\alpha v^\beta)\nabla_\beta\Phi$, where v^α is the particle's velocity vector, and the self-force is

$$\mathfrak{f}_\alpha = \mathfrak{m}\big(\delta_\alpha^{\ \beta} + v_\alpha v^\beta\big)\nabla_\beta\delta\Phi, \tag{1.3}$$

where $\delta\Phi$ is the perturbation created by the particle itself (which must be regularized before it is evaluated on the world line). For a circular orbit the self-force features two independent components. The first is $\mathfrak{f}_\phi$, which is responsible for all dissipative aspects and drives the particle's inspiral; the second is $\mathfrak{f}_r$, which provides a conservative correction to the relation between Ω and r_0. These components of the self-force are displayed in Fig. 2. We see the resonances at work in the dramatic excursions of the self-force from the typical nonresonant value. A resonance is produced whenever $\Omega = \mathrm{Re}(\omega)/m$, where ω is the eigenfrequency of a quasinormal mode of multipole order ℓ, and $m \leq \ell$ is an integer. Most resonances are extremely narrow; this is a consequence of the long lifetimes of the associated quasinormal modes. A notable exception is the resonance with the $\ell = 2$ fundamental mode of the fluid, at $r_0/R \simeq 1.38$, which is broad. We were able to associate each resonant feature in the self-force with a specific quasinormal mode; our discussion in Sec. VI provides these details.

The self-force is next incorporated (also in Sec. VI) into the particle's equations of motion, in an approximate treatment that assumes that the orbital evolution proceeds on a time scale that is long compared with the orbital period. The impact of the self-force can be seen in Fig. 3. The blue dashed line in the figure represents an evolution that incorporates only $\mathfrak{f}_\phi$, the dissipative component of the self-force. We see that Ω increases with time, which reflects the decreases in orbital radius that accompanies a radiative loss of orbital energy. The rate of increase is much larger

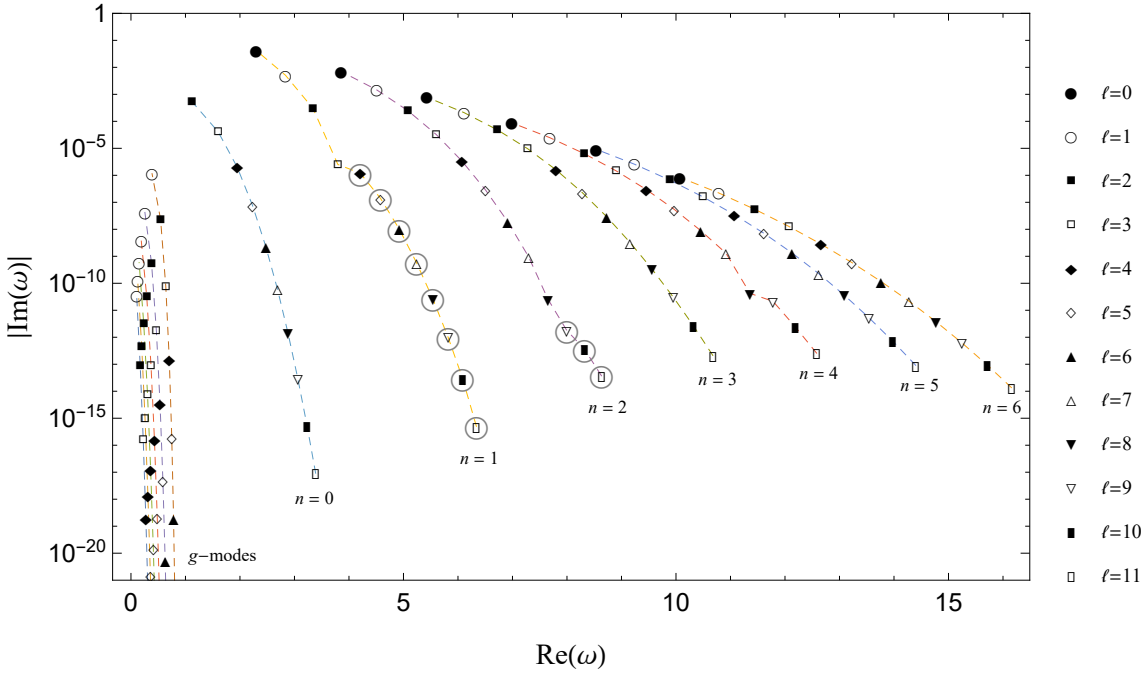

FIG. 1. Quasinormal modes of a fluid body with compactness $M/R = 0.3$ in the scalar theory of gravity presented in the main text. The modes are characterized by the real and imaginary parts of the eigenfrequency ω, which are presented in units of $\sqrt{M/R^3}$. The modes are labelled by values of the multipole order ℓ and the number $|n|$ of nodes of ξ_r, the radial component of the Lagrangian displacement vector. The modes with $n = 0$ are fundamental modes (f-modes), those with $n > 0$ are pressure modes (p-modes), and those with $n < 0$ are gravity modes (g-modes). The modes enclosed by circles are unstable, with $\mathrm{Im}(\omega) > 0$.

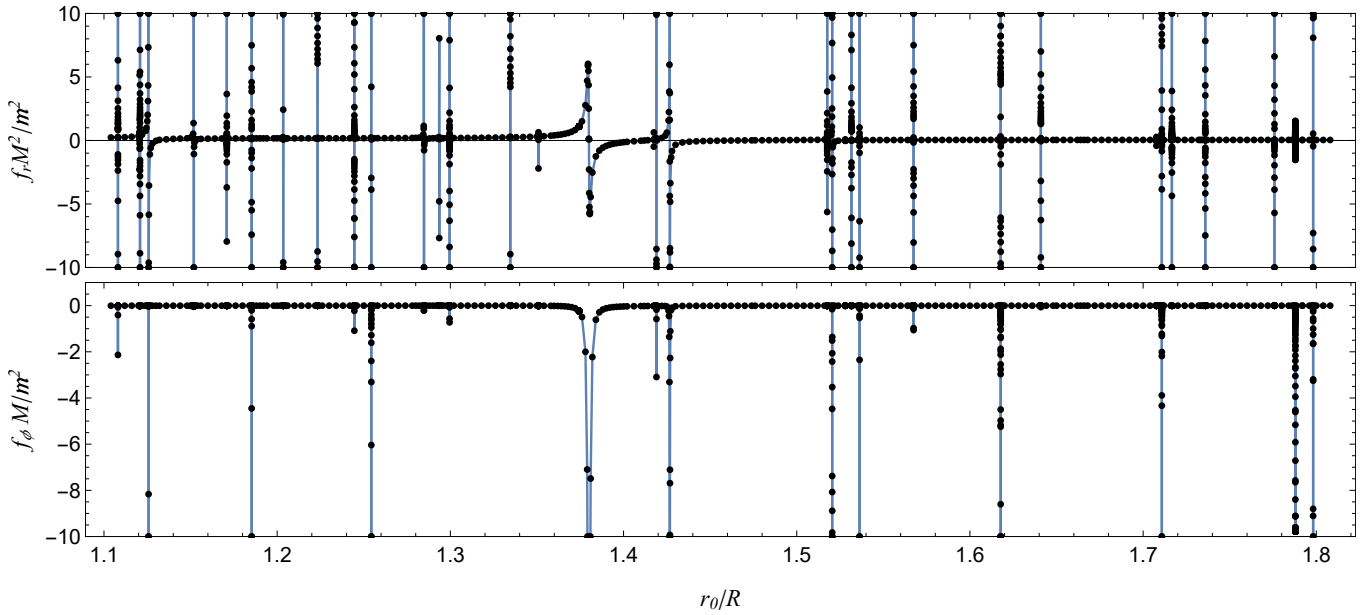

FIG. 2. Self-force on a particle of mass $\mathfrak{m}$ placed on a circular orbit of radius r_0 around a star with compactness $M/R = 0.3$. The radial component (upper panel) is presented in units of $\mathfrak{m}^2/M^2$, and the angular component (lower panel) in units of $\mathfrak{m}^2/M$. The orbital radius is displayed in units of the stellar radius R, for the range $1.10 < r_0/R < 1.81$. We see multiple resonances producing large excursions of the self-force from its typical nonresonant value (which is of the order of 10^{-2} for $\mathfrak{f}_r M^2/\mathfrak{m}^2$, and 10^{-3} for $\mathfrak{f}_\phi M/\mathfrak{m}^2$).

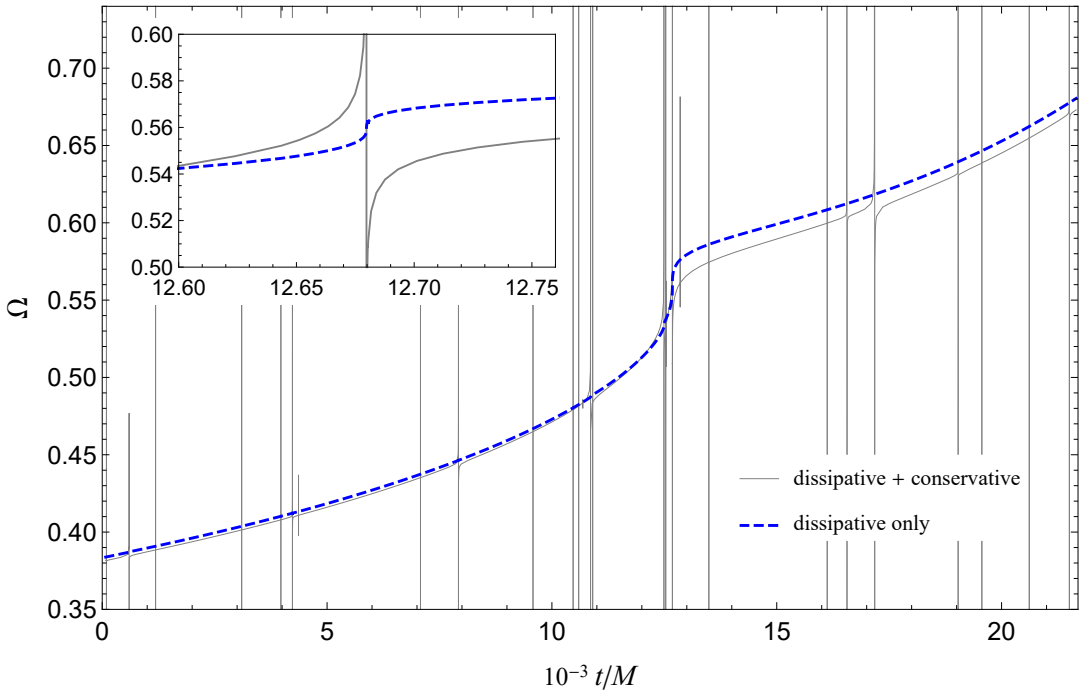

FIG. 3. Orbital angular velocity as a function of time resulting from the action of the self-force. The angular velocity is presented in units of $\sqrt{M/R^3}$, time is presented in units of M, and the orbital evolution was calculated for $\mathfrak{m}/M = 0.01$. The particle is initially set at $r_0 = 1.80$ when $t = 0$ and evolves until it reaches $r_0 = 1.20$. The dashed blue line represents an evolution that incorporates only $\mathfrak{f}_\phi$, the dissipative component of the self-force. The solid gray line represents an evolution calculated with both $\mathfrak{f}_r$ and $\mathfrak{f}_\phi$, and which therefore includes also the conservative component of the self-force. The inset highlights the interval around $t/M = 12,680$, when the particle crosses the broad resonance at $r_0/R \simeq 1.38$.

near $t/M \simeq 12,680$, and this corresponds to the particle crossing the broad resonance at $r_0/R \simeq 1.38$. The solid gray line represents an evolution calculated with both $\mathfrak{f}_\phi$ and $\mathfrak{f}_r$, and which therefore incorporates also the conservative aspects of the self-force. We see that $\mathfrak{f}_r$ produces large excursions around the purely dissipative evolution. As the particle enters a resonance, the angular frequency increases extremely rapidly, then decreases, and finally increases again to rejoin the dissipative evolution. These features are extremely narrow, reflecting again the long lifetimes of the associated quasinormal modes. An exception occurs with the broad resonance at $r_0/R \simeq 1.38$, where we see the same cycle of increase, decrease, and re-increase, but where we don't see the full evolution rejoining the dissipative evolution. We observe instead that the dissipative evolution over-estimates the angular frequency by a few percent as the particle comes out of the resonance. The mismatch between the actual and dissipative angular frequencies observed in Fig. 3 creates a dephasing $\Delta\phi$ between the two evolutions. We plot this as a function of time in Fig. 4, and the figure reveals that the dephasing indeed becomes significant over the inspiral time scale.

Except for the broad resonance near $r_0/R \simeq 1.38$, the resonant features observed in the self-force and the resulting orbital evolution are all extremely narrow, a consequence of the long lifetimes of the associated quasinormal modes. Nevertheless, these features can in principle be measured; in particular, the sudden excursions of the angular frequency around the smooth, dissipative curve would have a manifestation in the gravitational waves emitted by the particle. In situations involving shorter lifetimes and broader resonances, it can be expected that the resonant features would reveal valuable information regarding the body's internal composition. We feel that our findings in this paper motivate a more thorough analysis carried out in full general relativity.

The rest of the paper is devoted to a detailed derivation of the results presented above, accompanied with a more complete discussion. To set the stage, we consider in Sec. II the simplest model of a resonant self-force, implicating Newtonian gravity and a fluid body with a uniform mass density (see also Refs. [35, 36] for related Newtonian analyses). In this language the self-force is the result of a dynamical tidal interaction between the particle and the body. As we shall see, many of the features of our relativistic model are captured by this simplest of models.

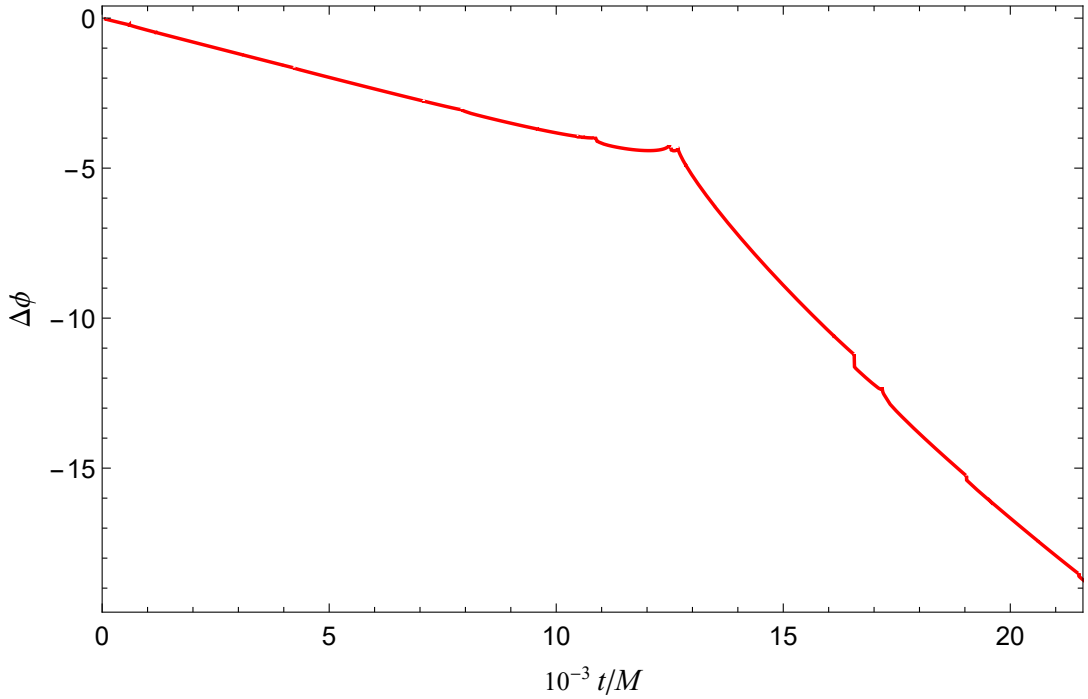

FIG. 4. Dephasing $\Delta\phi = \phi - \phi_0$ of the actual orbital evolution, given by $\phi(t)$, relative to the purely dissipative evolution, given by $\phi_0(t)$, as a function of time. We see that after the broad resonance at $r_0/R \simeq 1.38$ is crossed (at $t/M = 12,680$), there is a perceptible increase in the rate of dephasing.

II. NEWTONIAN MODEL OF RESONANT SELF-FORCE

As stated, the resonant features described previously in the scalar-gravity self-force can be captured by a strictly Newtonian model. In this situation a particle of mass $\mathfrak{m} \ll M$ raises a dynamical tide on a fluid body of mass M and radius R, and the resulting deformation of the body's gravitational potential acts back on the particle, thereby producing what can be described as a self-force. For simplicity we take the unperturbed configuration to be a spherical fluid distribution of uniform mass density, and we truncate the tidal interaction at the leading, quadrupole order. In this simplified model the tidal interaction is mediated entirely by the f-mode of the fluid's quadrupolar perturbation. The Newtonian physics of dynamical tides is reviewed in Sec. 2.5.3 of Ref. [37], and we shall import results and notation from this reference.

A. Tidal dynamics

The dynamical tide is driven by the particle's gravity, which is described in terms of the Newtonian potential $U_{\rm part}(t, \boldsymbol{x})$; the spatial coordinates $\boldsymbol{x}$ measure a displacement away from the body's center-of-mass. The tidal interaction can be developed as a multipole expansion, and at the leading order, the tidal environment is described by the tidal quadrupole-moment tensor $\mathcal{E}_{ab}(t) := -\partial_{ab} U_{\rm part}(t, \mathbf{0})$, in which the particle's potential is evaluated at $\boldsymbol{x} = \mathbf{0}$ after differentiation. The body's tidal response is measured by $I_{ab}(t)$, the quadrupole-moment tensor of its mass distribution (defined as a tracefree tensor). This is given by

$$I_{ab} = -\frac{2}{5} M R^2 \mathcal{F}_{ab}, \tag{2.1}$$

where

$$\mathcal{F}_{ab}(t) := \frac{1}{\omega} \int_{-\infty}^{t} \mathcal{E}_{ab}(t') e^{-\kappa(t-t')} \sin\omega(t-t')\, dt' \tag{2.2}$$

is the fluid's response function; the real part of the mode frequency is denoted ω, and its imaginary part is denoted $-\kappa$. The discussion in Ref. [37] excludes dissipation, and as a consequence, the exponential factor does not appear

in their Eq. (2.290). It was inserted here to incorporate a source of dissipation within the system. In the relativistic model examined below, dissipation is naturally exhibited and associated with the emission of gravitational radiation; here it is inserted by hand, and associated with viscosity acting within the body. For the quadrupole f-mode of a fluid with uniform density, $\omega^2 = 4M/(5R^3)$. We assume that $\kappa \ll \omega$ to reproduce the long lifetimes of the relativistic quasinormal modes; we explicitly assume that $\kappa > 0$, so that the f-mode is stable.

We take the particle to move on a circular orbit of radius r and angular velocity $\Omega = \sqrt{M/r^3}$ around the fluid body. For this situation we have

$$\mathcal{E}_{ab} = -\frac{3\mathfrak{m}}{r^3} n_{\langle ab\rangle}, \tag{2.3}$$

where $n_{\langle ab\rangle} := n_a n_b - \frac{1}{3}\delta_{ab}$ is a symmetric tracefree tensor formed from

$$\boldsymbol{n} := (\cos\phi, \sin\phi, 0), \tag{2.4}$$

a unit vector that points from the body's center-of-mass to the particle, at which $\phi = \Omega t$. The coordinate system is oriented in such a way that the orbital motion takes place in the x-y plane. For subsequent calculations it is necessary to complete the vectorial basis with

$$\boldsymbol{\lambda} := (-\sin\phi, \cos\phi, 0); \qquad \boldsymbol{e} := (0, 0, 1). \tag{2.5}$$

The unit vector $\boldsymbol{\lambda}$ points in the direction of the particle's velocity, and $\boldsymbol{e}$ is normal to the orbital plane.

Inserting Eq. (2.3) into Eq. (2.2) and performing the integration returns

$$\mathcal{F}_{ab} = \frac{15}{4}\frac{\mathfrak{m}}{M}\left(\frac{R}{r}\right)^3 \Big[2A n_{(a}\lambda_{b)} - 2B n_{\langle ab\rangle} + (3C - B) e_{\langle ab\rangle}\Big], \tag{2.6}$$

where

$$A := \frac{2\kappa\omega^2\Omega}{\big[(\omega - 2\Omega)^2 + \kappa^2\big]\big[(\omega + 2\Omega)^2 + \kappa^2\big]}, \tag{2.7a}$$

$$B := \frac{\frac{1}{2}\omega^2\big(\omega^2 - 4\Omega^2 + \kappa^2\big)}{\big[(\omega - 2\Omega)^2 + \kappa^2\big]\big[(\omega + 2\Omega)^2 + \kappa^2\big]}, \tag{2.7b}$$

$$C := \frac{\omega^2}{6(\omega^2 + \kappa^2)}. \tag{2.7c}$$

These expressions reveal that a resonance occurs when $2\Omega = \omega$; the factor of two is associated with the quadrupolar nature of the tidal interaction. The width of the resonant features is determined by κ, the inverse of the damping time. Equation (2.6) can be inserted into Eq. (2.1) to obtain the body's quadrupole-moment tensor. (Strictly speaking, the integration from $t' = -\infty$ to $t' = t$ in Eq. (2.2) does not converge, because the particle is assumed to be at all times on a fixed circular orbit. This defect can be remedied by choosing the lower bound to be some finite reference time t_0. The resulting dependence of $\mathcal{F}_{ab}$ on t_0 can then be shown to correspond to a transient response that decays exponentially. The expression shown above corresponds to the steady-state response that emerges when $t \gg t_0$.)

B. Self-force

The tide produces a deformation of the body's gravitational potential, which is otherwise given by $U = M/r$. According to Eq. (1.149) of Ref. [37], the perturbation is described by

$$\delta U = \frac{1}{2} I^{ab}\partial_{ab}\left(\frac{1}{r}\right) \tag{2.8}$$

when it is truncated to the leading, quadrupole order. This perturbation contributes a force $\mathfrak{f}_a = \mathfrak{m}\partial_a \delta U$ acting on the particle, and this shall be our Newtonian model for the self-force. The self-force is to be added to the original force $\mathfrak{m}\partial_a U$ created by the body, which is responsible for maintaining the circular orbit. A straightforward computation, making use of Eq. (2.1) as well as Eq. (1.152c) of Ref. [37], returns

$$\mathfrak{f}_a = -\frac{1}{5}\mathfrak{m}MR^2\mathcal{F}^{bc}\partial_{abc}\left(\frac{1}{r}\right) = 3\mathfrak{m}M\frac{R^2}{r^4}\mathcal{F}^{bc}n_{\langle abc\rangle}, \tag{2.9}$$

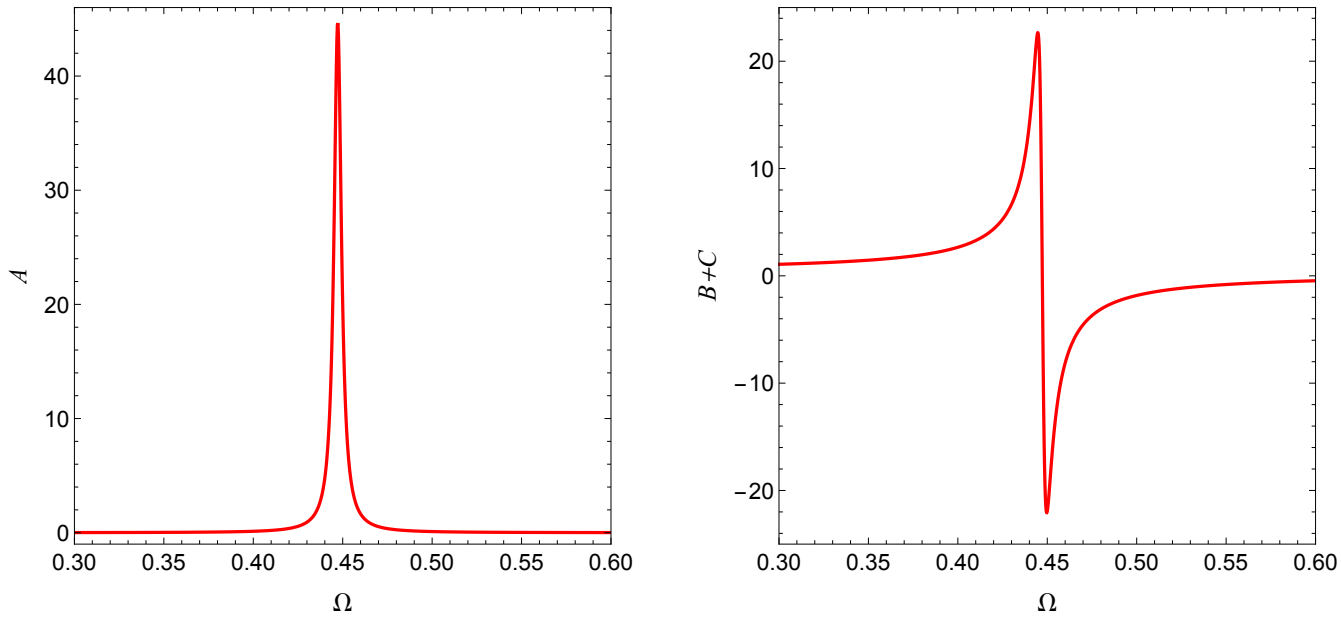

FIG. 5. Plots of A and $B+C$ as a function of Ω. The orbital frequency is presented in units of $\sqrt{M/R^3}$, and the resonance occurs when $\Omega = \frac{1}{2}\omega \simeq 0.447$. The damping parameter is set to $\kappa = 0.005$, in the same frequency units.

where $n_{\langle abc\rangle} := n_a n_b n_c - \frac{1}{5}(n_a\delta_{bc} + n_b\delta_{ac} + n_c\delta_{ab})$. Inserting Eq. (2.6) and performing the tensorial manipulations yields

$$\mathfrak{f} = -\frac{9}{4}\frac{\mathfrak{m}^2 R^5}{r^7}\Big[3(B+C)\boldsymbol{n} + 2A\boldsymbol{\lambda}\Big]. \tag{2.10}$$

The self-force features a radial component proportional to $B+C$, and a tangential component proportional to A; these functions of the orbital frequency Ω are plotted in Fig. 5. The radial component of the self-force is associated with conservative effects, while its tangential component is associated with dissipative effects. The components of the Newtonian self-force, $\mathfrak{f}_r \propto -(B+C)$ and $\mathfrak{f}_\phi \propto -A$, can be compared across a resonance to those of the relativistic self-force in Fig. 2. We have qualitative agreement, and in fact, we have verified that the Newtonian expressions provide excellent fits of each resonant feature when ω and κ are matched to the relevant quasinormal mode.

C. Orbital evolution

We next wish to describe the impact of the self-force on the motion of the particle. The equations of motion are $\boldsymbol{F} = \mathfrak{m}\boldsymbol{a}$, where $\boldsymbol{F}$ is the total force acting on the particle, and

$$\boldsymbol{a} = \big(\ddot{r} - r\Omega^2\big)\boldsymbol{n} + \frac{1}{r}\frac{d}{dt}\big(r^2\Omega\big)\boldsymbol{\lambda} \tag{2.11}$$

is the acceleration vector; $\Omega := \dot{\phi}$, and an overdot indicates differentiation with respect to t. To formalize the fact that the self-force is small compared with the force produced by the unperturbed body, we introduce a small parameter $\epsilon \ll 1$ and expand the total force in powers of ϵ,

$$\boldsymbol{F} = \boldsymbol{F}_0 + \epsilon\boldsymbol{F}_1 + O(\epsilon^2). \tag{2.12}$$

Here $\boldsymbol{F}_0 = -\mathfrak{m}M\boldsymbol{n}/r^2$ and $\epsilon\boldsymbol{F}_1 = \mathfrak{f}$. We assume that the particle follows a circular orbit that changes very slowly as a result of the self-force. To formalize this assumption we follow Pound's multiscale methods (see Sec. IV of Ref. [38]) and introduce a slow-time variable $\bar{t} := \epsilon t$, and state that the orbital radius r and the angular frequency Ω shall be functions of $\bar{t}$; quantities (such as the velocity vector) that vary over the orbital time scale are written as functions of the fast-time variable t. We assume also that the orbital frequency admits an expansion in powers of ϵ:

$$\Omega = \Omega_0(\bar{t}) + \epsilon\Omega_1(\bar{t}) + O(\epsilon^2). \tag{2.13}$$

To obtain a description of the perturbed motion we insert these functional relations into the equations of motion (writing, for example, $\dot{r} = \epsilon r'$, with a prime indicating differentiation with respect to $\bar{t}$), and we expand in powers of ϵ. The radial component becomes

$$\mathfrak{m}\big(r\Omega_0^2 + 2\epsilon r\Omega_0\Omega_1\big) = \mathfrak{m}M/r^2 - \epsilon \boldsymbol{F}_1 \cdot \boldsymbol{n} + O(\epsilon^2), \tag{2.14}$$

while the tangential component becomes

$$\epsilon\mathfrak{m}\big(r\Omega_0' + 2\Omega_0 r'\big) = \epsilon \boldsymbol{F}_1 \cdot \boldsymbol{\lambda} + O(\epsilon^2). \tag{2.15}$$

At order ϵ^0 we recover the relation $\Omega_0^2 = M/r^3$, which implies that $r'/r = -(2/3)\Omega_0'/\Omega_0$. At order ϵ the radial equation produces

$$\Omega_1 = -\frac{1}{2\mathfrak{m}r\Omega_0}\boldsymbol{F}_1 \cdot \boldsymbol{n}, \tag{2.16}$$

while the tangential equation gives rise to

$$\Omega_0' = -\frac{3}{\mathfrak{m}r}\boldsymbol{F}_1 \cdot \boldsymbol{\lambda}. \tag{2.17}$$

These are the required evolution equations. To display them in their final form we eliminate $\bar{t}$ in favor of t and re-express $\boldsymbol{F}_1$ in terms of the self-force $\mathfrak{f}$. We obtain the complete set of equations

$$\Omega = \Omega_0 - \frac{1}{2\mathfrak{m}r\Omega_0}\mathfrak{f} \cdot \boldsymbol{n}, \tag{2.18a}$$

$$\frac{d\Omega_0}{dt} = -\frac{3}{\mathfrak{m}r}\mathfrak{f} \cdot \boldsymbol{\lambda}, \tag{2.18b}$$

$$\Omega_0^2 = \frac{M}{r^3}. \tag{2.18c}$$

One sees that in this approximate description of the motion, the radial component of the self-force produces a shift in angular frequency with respect to Ω_0, and that the tangential component drives an evolution of Ω_0 (and therefore of r).

In our current application the self-force is given by Eq. (2.10), and the evolution equations become

$$\Omega = \Omega_0 + \frac{27}{8}\frac{\mathfrak{m}R^5}{\Omega_0 r^8}(B + C), \tag{2.19a}$$

$$\frac{d\Omega_0}{dt} = \frac{27}{2}\frac{\mathfrak{m}R^5}{r^8}A. \tag{2.19b}$$

Before integrating these equations it is convenient to rescale the variables so as to make them dimensionless. We shall therefore measure all frequencies in units of $\Omega^* := \sqrt{M/R^3}$, measure time in units of $t^* := (M/\mathfrak{m})\sqrt{R^3/M}$, and measure r in units of R. In these natural units integration yields

$$t = t_i + \frac{2}{27}\frac{1}{\kappa\omega^2}\left\{\frac{1}{\Omega_i^{16/3}}\left[\frac{3}{32}(\omega^2+\kappa^2)^2 - \frac{6}{5}(\omega^2-\kappa^2)\Omega_i^2 + 6\Omega_i^4\right]\right.$$
$$\left. - \frac{1}{\Omega_0^{16/3}}\left[\frac{3}{32}(\omega^2+\kappa^2)^2 - \frac{6}{5}(\omega^2-\kappa^2)\Omega_0^2 + 6\Omega_0^4\right]\right\}, \tag{2.20a}$$

$$\Omega = \Omega_0 + \frac{27}{8}\frac{\mathfrak{m}}{M}\Omega_0^{13/3}(B + C), \tag{2.20b}$$

where t_i is the time at which $\Omega_0 = \Omega_i$. These equations provide a parametric expression for $\Omega(t)$, with Ω_0 playing the role of parameter.

A plot of the angular frequency is presented in Fig. 6. The dashed blue curve represents $\Omega_0(t)$, which changes with time by purely dissipative effects; the change is slow off resonance, and rapid near resonance. The solid gray curve represents $\Omega(t)$, which also includes the shift produced by the conservative piece of the self-force. The shift is positive before resonance, and negative just after it. The inset shows the details of resonance crossing, with the rapid increase of $\Omega(t)$ immediately prior to resonance, the very sudden decrease at resonance, and the rapid final increase

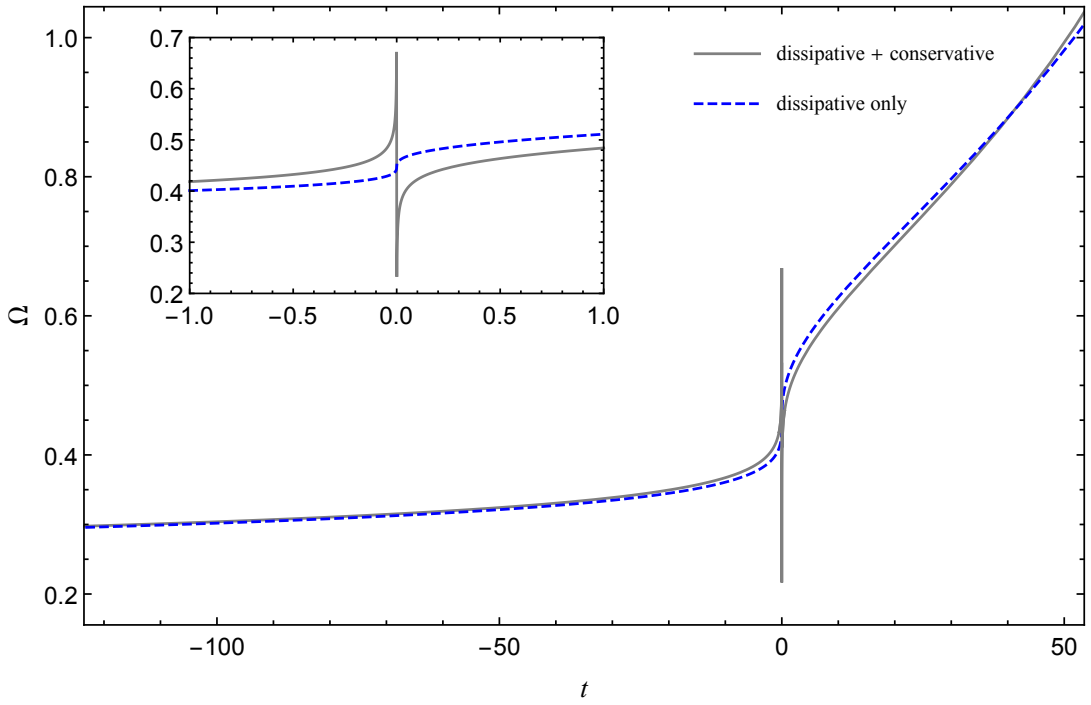

FIG. 6. Plot of the angular velocity Ω as a function of time. The frequency is presented in units of $\sqrt{M/R^3}$, and the resonance occurs when $\Omega = \frac{1}{2}\omega \simeq 0.447$. The damping parameter is set to $\kappa = 0.005$, in the same frequency units. Time is presented in units of $(M/\mathfrak{m})\sqrt{R^3/M}$, and the zero of time coincides with resonance crossing. The mass ratio was set to $\mathfrak{m}/M = 0.1$ to ensure that the curves can be distinguished.

immediately after resonance. Figure 6 can be compared with its relativistic version in Fig. 3; we again find excellent qualitative agreement.

The radial (conservative) component of the self-force produces a shift $\Delta\Omega := \Omega - \Omega_0$ of the angular frequency relative to Ω_0, which evolves by sole virtue of the tangential (dissipative) component of the self-force. This shift produces a dephasing $\Delta\phi$ of the orbit relative to the purely dissipative evolution. The dephasing per frequency interval is given by

$$\frac{d\Delta\phi}{d\Omega_0} = \frac{d\Delta\phi/dt}{d\Omega_0/dt} = \frac{\Delta\Omega}{d\Omega_0/dt}, \tag{2.21}$$

and this evaluates to

$$\frac{d\Delta\phi}{d\Omega_0} = \frac{B+C}{4\Omega_0 A} = \frac{\omega^2+\kappa^2}{12\kappa\Omega_0^2} - \frac{5\omega^2+\kappa^2}{12\kappa(\omega^2+\kappa^2)} + \frac{\Omega_0^2}{3\kappa(\omega^2+\kappa^2)}. \tag{2.22}$$

The total dephasing across the resonance can be obtained by integrating this expression over the frequency interval $\frac{1}{2}\omega - \kappa < \Omega_0 < \frac{1}{2}\omega + \kappa$, with κ providing a measure of the width of the resonance. A simple calculation shows that the total dephasing amounts to $\frac{73}{18}(\kappa/\omega)^2$ when $\kappa/\omega \ll 1$. This is small, which was to be expected from the fact that the large increase in angular velocity witnessed immediately before and after resonance is almost completely cancelled by the rapid decrease during resonance.

III. SCALAR GRAVITY COUPLED TO A PERFECT FLUID

In this section we introduce the scalar theory of gravity adopted in this work. The theory is inspired from scalar-tensor theories of gravity, in which we simply make the tensor component of the gravitational field nondynamical. The theory, in fact, is identical to the venerable Nordström theory, which is conveniently reviewed in Ref. [39].

The field equation for the gravitational field Φ and the equations of motion for the matter fields are initially formulated in a curved spacetime with a nondynamical metric $g_{\alpha\beta}$, and they are postulated to be of the form

$$\Box\Phi = 4\pi\alpha(\Phi)T^{\mu}_{\ \mu}, \qquad \nabla_\beta T^{\alpha\beta} = -\alpha(\Phi)T^{\mu}_{\ \mu}\nabla^\alpha\Phi, \tag{3.1}$$

in which $\Box := g^{\alpha\beta}\nabla_\alpha\nabla_\beta$ is the covariant wave operator, $\alpha(\Phi)$ is an arbitrary function of the scalar potential, and $T^{\alpha\beta}$ is the energy-momentum tensor of the matter fields.

The field and matter equations (3.1) can be derived on the basis of a variational principle. Consider the action

$$S = \frac{1}{16\pi}\int d^4x\sqrt{-g}\,\big(\mathrm{R} - 2g^{\alpha\beta}\nabla_\alpha\Phi\nabla_\beta\Phi\big) + S_m[\Psi_m, \beta(\Phi)g_{\alpha\beta}], \tag{3.2}$$

where $g := \det(g_{\alpha\beta})$, R is the Ricci scalar, and S_m is the action of the matter fields, which are collectively denoted by Ψ_m and couple to the conformally rescaled metric $\tilde{g}_{\alpha\beta} := \beta(\Phi)g_{\alpha\beta}$, with $\beta(\Phi)$ an arbitrary function of Φ. Variation with respect to $g_{\alpha\beta}$ yields

$$G^{\alpha\beta} - 2\nabla^\alpha\Phi\nabla^\beta\Phi + g^{\alpha\beta}\nabla_\mu\Phi\nabla^\mu\Phi = 8\pi T^{\alpha\beta}, \tag{3.3}$$

where $T^{\alpha\beta} := (2/\sqrt{-g})\delta S_m[\Phi_m, \beta(\Phi)g_{\mu\nu}]/\delta g_{\alpha\beta}$. Variation with respect to the scalar field gives

$$\Box\Phi = -2\pi\frac{d\ln\beta(\Phi)}{d\Phi}T^\mu_{\ \mu}, \tag{3.4}$$

which is the field equation displayed in Eq. (3.1) upon identifying $\alpha = -(1/2)d\ln\beta/d\Phi$. Taking the divergence of Eq. (3.3), and making use of Eq. (3.4), one obtains the equations of motion for the matter fields shown in Eq. (3.1). Notice, from Eq. (3.3), that the field equations admit a conserved total energy-momentum tensor, the sum of $T^{\alpha\beta}$ and

$$t^{\alpha\beta} := \frac{1}{4\pi}\Big(\nabla^\alpha\Phi\nabla^\beta\Phi - \frac{1}{2}g^{\alpha\beta}\nabla_\mu\Phi\nabla^\mu\Phi\Big), \tag{3.5}$$

which can be interpreted as the energy-momentum tensor of the gravitational field. The construction above parallels the Einstein-frame formulation of scalar-tensor theories [40], which are viable theories of gravity for some range of coupling functions. On the other hand, in our simplified model we take Eqs. (3.1) as the starting point, assuming a fixed nondynamical background metric.

We now consider a perfect fluid with rest-mass density ρ, pressure p, density of internal energy ϵ, total energy density $\mu = \rho + \epsilon$, and velocity u^α coupled to the scalar gravitational field Φ. With

$$T^{\alpha\beta} = \mu u^\alpha u^\beta + pP^{\alpha\beta}, \qquad P^{\alpha\beta} = g^{\alpha\beta} + u^\alpha u^\beta, \tag{3.6}$$

the field and fluid equations (3.1) take the explicit form

$$0 = S := \Box\Phi + 4\pi\alpha(\mu - 3p), \tag{3.7a}$$

$$0 = S' := u^\alpha\nabla_\alpha\mu + (\mu + p)\nabla_\alpha u^\alpha + \alpha(\mu - 3p)u^\alpha\nabla_\alpha\Phi, \tag{3.7b}$$

$$0 = S_\alpha := (\mu + p)a_\alpha + P_\alpha^{\ \beta}\nabla_\beta p - \alpha(\mu - 3p)P_\alpha^{\ \beta}\nabla_\beta\Phi, \tag{3.7c}$$

where $a_\alpha := u^\beta\nabla_\beta u_\alpha$ is the fluid's covariant acceleration. To these equations we adjoin an equation of state $p = p(\rho, s)$, $\epsilon = \epsilon(\rho, s)$, in which s is the fluid's specific entropy (entropy per unit mass), and the statement of rest-mass conservation,

$$\nabla_\alpha\big(\rho u^\alpha\big) = 0. \tag{3.8}$$

Equation (3.7b) can then be expressed in the form of a dynamical version of the first law of thermodynamics,

$$\rho T\frac{ds}{d\tau} = \frac{d\epsilon}{d\tau} - \frac{\epsilon + p}{\rho}\frac{d\rho}{d\tau} = \frac{d\mu}{d\tau} - \frac{\mu + p}{\rho}\frac{d\rho}{d\tau} = -\alpha(\mu - 3p)\frac{d\Phi}{d\tau}, \tag{3.9}$$

where T is the fluid's temperature and τ is proper time on the world line of each fluid element. We see that the gravitational field is a source of heat when the fluid configuration depends on time.

In the sequel we shall simplify the formulation of the theory by setting

$$\alpha(\Phi) = 1, \qquad g_{\alpha\beta} = \eta_{\alpha\beta}, \tag{3.10}$$

in which $\eta_{\alpha\beta}$ is the Minkowski metric in the selected coordinate system (which may not be the standard Lorentzian coordinates). In this formulation the theory of gravity is linear, and the background geometry is flat.

IV. STELLAR MODELS

With the choice made in Eq. (3.10) we consider static and spherically-symmetric configurations of the fluid and gravitational field. Adopting spherical polar coordinates (t, r, θ, ϕ) and letting $u^\alpha = (1, 0, 0, 0)$, $a_\alpha = 0$, we find that the field and fluid equations reduce to the system

$$\frac{dm}{dr} = 4\pi r^2(\mu - 3p), \tag{4.1a}$$

$$\frac{d\Phi}{dr} = -\frac{m(r)}{r^2}, \tag{4.1b}$$

$$\frac{dp}{dr} = (\mu - 3p)\frac{d\Phi}{dr} = -(\mu - 3p)\frac{m(r)}{r^2}, \tag{4.1c}$$

in which an effective mass function $m(r)$ was introduced as an auxiliary variable. The structure equations closely resemble the Newtonian equations, with the effective mass density $\mu - 3p = \rho + \epsilon - 3p$ replacing the rest-mass density ρ. The equations guarantee that $m(r) = M =$ constant outside the body, where the potential is given by $\Phi = M/r$.

A particularly simple stellar structure follows if we postulate the relation $p = K(\rho + \epsilon - 3p)^2$ between the pressure and the effective mass density, where K is a constant; this is a slight modification of the $n = 1$ polytropic model described by $p = K\rho^2$. This modified assignment gives rise to a physically acceptable, zero-temperature equation of state, which we now write as $\rho = \rho(p)$ and $\epsilon = \epsilon(p)$.

The expression for ϵ can be found by integrating $d\epsilon = (\epsilon + p)\rho^{-1}\, d\rho$ with $\rho = \sqrt{p/K} - \epsilon + 3p$. This yields

$$\rho = \sqrt{\frac{p}{K}}\sqrt{1 + 4x}, \tag{4.2a}$$

$$\epsilon = 3p + \sqrt{\frac{p}{K}}\Big(1 - \sqrt{1 + 4x}\Big), \tag{4.2b}$$

with $x := \sqrt{Kp}$. The speed of sound associated with this equation of state is given by

$$c_s^2 = \frac{dp}{d\mu} = \frac{2x}{1 + 6x} < \frac{1}{3}. \tag{4.3}$$

When x is small the equation of state reduces to $\rho = \sqrt{p/K}[1 + 2x + O(x^2)]$ and $\epsilon = p[1 + 2x + O(x^2)]$, and it deviates little from a polytropic equation of state with $n = 1$.

The solution to the structure equations (4.1) for this equation of state can be expressed as

$$p = \frac{\pi M^2}{8R^4}\left[\frac{\sin(\pi r/R)}{\pi r/R}\right]^2, \tag{4.4a}$$

$$\rho = \frac{\pi M}{4R^3}\frac{\sin(\pi r/R)}{\pi r/R}\sqrt{1 + \frac{2M}{R}\frac{\sin(\pi r/R)}{\pi r/R}}, \tag{4.4b}$$

$$\mu = \frac{\pi M}{4R^3}\frac{\sin(\pi r/R)}{\pi r/R}\left[1 + \frac{3M}{2R}\frac{\sin(\pi r/R)}{\pi r/R}\right], \tag{4.4c}$$

$$m = M\frac{r}{R}\left[\frac{\sin(\pi r/R)}{\pi r/R} - \cos(\pi r/R)\right]; \tag{4.4d}$$

the constant K is related to the stellar radius R by $K = (2/\pi)R^2$. The pressure is largest at the center of the star, where it is equal to $p_c = \pi M^2/(8R^4)$. For future reference we record that

$$\Gamma := \frac{\rho}{p}\frac{dp/dr}{d\rho/dr} = 2\frac{\pi r + 2M\sin(\pi r/R)}{\pi r + 3M\sin(\pi r/R)}. \tag{4.5}$$

This function increases monotonically with r, and it is bounded by

$$\Gamma(r = 0) = 2\frac{1 + 2M/R}{1 + 3M/R} \le \Gamma(r) \le 2 = \Gamma(r = R). \tag{4.6}$$

V. FLUID PERTURBATIONS

In this section we consider perturbations of the equilibrium stellar model of Sec. IV and describe the quasinormal modes of the fluid-gravity system.

A. Formalism

The unperturbed state of the fluid is taken to be an equilibrium for which $u^\alpha = (1,0,0,0)$, $a_\alpha = 0$, and all fluid variables are independent of time. The perturbation, however, is allowed to depend on time. We continue to work in Minkowski spacetime, but keep the equations covariant in order to retain the freedom to choose the coordinate system. We rely on the Lagrangian theory of fluid perturbations reviewed in Ref. [41], and import many relevant results from this reference. We recall that for any fluid variable Q, scalar or tensorial, the Lagrangian perturbation ΔQ and Eulerian perturbation δQ are related by $\Delta Q = \delta Q + \mathcal{L}_\xi Q$, in which $\mathcal{L}_\xi$ is the Lie derivative in the direction of the Lagrangian displacement vector ξ^α.

As derived in Sec. 2.2 of Ref. [41], the Lagrangian perturbation of the velocity vector is given by

$$\Delta u^\alpha = \frac{1}{2} u^\alpha u^\beta u^\gamma \Delta\eta_{\beta\gamma}, \tag{5.1}$$

while the perturbation of the rest-mass density is

$$\Delta\rho = -\frac{1}{2}\rho P^{\alpha\beta}\Delta\eta_{\alpha\beta}. \tag{5.2}$$

In our case there is no Eulerian perturbation of the metric, and $\Delta\eta_{\alpha\beta} = \nabla_\alpha\xi_\beta + \nabla_\beta\xi_\alpha$.

To derive an expression for $\Delta\mu$ we rely on the dynamical formulation of the first law of thermodynamics, Eq. (3.9), which becomes

$$0 = \Delta\frac{d\mu}{d\tau} - \frac{\mu+p}{\rho}\,\Delta\frac{d\rho}{d\tau} + (\mu - 3p)\Delta\frac{d\Phi}{d\tau} \tag{5.3}$$

after the perturbation; the terms proportional to $d\rho/d\tau$ and $d\Phi/d\tau$ were eliminated because these quantities vanish in the unperturbed state. The commutation relation

$$\left[\Delta, \frac{d}{d\tau}\right] f = \frac{1}{2}\frac{df}{d\tau} u^\alpha u^\beta\, \Delta\eta_{\alpha\beta}, \tag{5.4}$$

where f is an arbitrary scalar, further implies that the first law can be written as

$$0 = \frac{d}{d\tau}\Delta\mu - \frac{\mu+p}{\rho}\,\frac{d}{d\tau}\Delta\rho + (\mu-3p)\frac{d}{d\tau}\Delta\Phi = \frac{d}{d\tau}\left[\Delta\mu - \frac{\mu+p}{\rho}\,\Delta\rho + (\mu-3p)\Delta\Phi\right]. \tag{5.5}$$

Integrating, we arrive at

$$\Delta\mu = \frac{\mu+p}{\rho}\,\Delta\rho - (\mu-3p)\Delta\Phi = -\frac{1}{2}(\mu+p)P^{\alpha\beta}\,\Delta\eta_{\alpha\beta} - (\mu-3p)\Delta\Phi, \tag{5.6}$$

where $\Delta\Phi = \delta\Phi + \xi^\alpha\nabla_\alpha\Phi$.

Turning next to Δp, we invoke the equation of state $p = p(\rho, s)$ to write

$$\begin{aligned}\frac{dp}{d\tau} &= \left(\frac{\partial p}{\partial\rho}\right)_s \frac{d\rho}{d\tau} + \left(\frac{\partial p}{\partial s}\right)_\rho \frac{ds}{d\tau} \\ &= \frac{\Gamma_1 p}{\rho}\,\frac{d\rho}{d\tau} + (\Gamma_3 - 1)\rho T\,\frac{ds}{d\tau} \\ &= \frac{\Gamma_1 p}{\rho}\,\frac{d\rho}{d\tau} - (\Gamma_3 - 1)(\mu - 3p)\,\frac{d\Phi}{d\tau},\end{aligned} \tag{5.7}$$

where

$$\Gamma_1 := \left(\frac{\partial \ln p}{\partial \ln\rho}\right)_s, \qquad \Gamma_3 - 1 := \left(\frac{\partial \ln T}{\partial \ln\rho}\right)_s \tag{5.8}$$

are the standard adiabatic exponents. To go from the first to the second line we invoked the Maxwell relation $(\partial p/\partial s)_\rho = \rho^2(\partial T/\partial\rho)_s$, and to go to the third line we used Eq. (3.9) to relate $ds/d\tau$ to $d\Phi/d\tau$. Perturbing and integrating the equation for $dp/d\tau$, as we did for $d\mu/d\tau$, we arrive at

$$\Delta p = \frac{\Gamma_1 p}{\rho}\,\Delta\rho - (\Gamma_3 - 1)(\mu - 3p)\Delta\Phi = -\frac{1}{2}\Gamma_1 p P^{\alpha\beta}\,\Delta\eta_{\alpha\beta} - (\Gamma_3 - 1)(\mu - 3p)\Delta\Phi. \tag{5.9}$$

Importing from Sec. 7.1 of Ref. [41] and keeping in mind that the unperturbed state is an equilibrium configuration, the Lagrangian perturbation of the acceleration vector is

$$\Delta a_\alpha = P_\alpha{}^\beta\left[u^\mu\mathcal{L}_u\Delta\eta_{\beta\mu} - \frac{1}{2}\nabla_\beta\big(u^\mu u^\nu\,\Delta\eta_{\mu\nu}\big)\right]. \tag{5.10}$$

We also have

$$\Delta P_\alpha{}^\beta = u^\beta P_\alpha{}^\gamma u^\delta\Delta\eta_{\gamma\delta} \tag{5.11}$$

and

$$\Delta\nabla_\beta p = \nabla_\beta\Delta p, \qquad \Delta\nabla_\beta\Phi = \nabla_\beta\Delta\Phi. \tag{5.12}$$

With all this we arrive at the perturbation of Euler's equation (3.7c),

$$0 = \Delta S_\alpha = P_\alpha{}^\beta\left[(\mu+p)\mathcal{L}_u\big(u^\mu\,\Delta\eta_{\beta\mu}\big) - \frac{1}{2}(\mu+p)\nabla_\beta\big(u^\mu u^\nu\,\Delta\eta_{\mu\nu}\big) + \nabla_\beta\Delta p - (\mu-3p)\nabla_\beta\Delta\Phi - (\Delta\mu - 3\Delta p)\nabla_\beta\Phi\right]. \tag{5.13}$$

The (Eulerian) perturbation of the gravitational field equation gives

$$0 = \delta S := \Box\delta\Phi + 4\pi(\delta\mu - 3\delta p), \tag{5.14}$$

and these equations govern the behavior of the perturbed configuration, as described by ξ^α and $\delta\Phi$.

B. Implementation

We take the unperturbed configuration to be static and spherically-symmetric, so that the body's structure is determined by Eqs. (4.1). The components of the Lagrangian displacement vector can be decomposed in a sum over modes, each of them of the form

$$\xi_t = 0, \qquad \xi_r = x(r)Y_{\ell m}(\theta,\phi)e^{-i\omega t}, \qquad \xi_A = z(r)\partial_A Y_{\ell m}(\theta,\phi)e^{-i\omega t}, \tag{5.15}$$

where the uppercase index $A = 1, 2$ runs over the angular coordinates $\theta^A = (\theta,\phi)$, and $Y_{\ell m}(\theta,\phi)$ are the usual spherical-harmonic functions; we have that z is undefined when $\ell = 0$. The Eulerian perturbation of the gravitational potential is similarly expressed as

$$\delta\Phi = P(r)Y_{\ell m}(\theta,\phi)e^{-i\omega t}. \tag{5.16}$$

In these equations, it is understood (but not shown) that the variables $\{x, z, P\}$ carry a multipole label ℓ and a frequency label ω; m is not required as a label because the unperturbed configuration is spherically-symmetric.

Substitution of these expressions into the perturbation equations $\Delta S_\alpha = 0$ and $\delta S = 0$ produces an explicit system of ordinary differential equations for the variables $\{x, z, P\}$. However, it turns out to be more convenient to formulate the perturbation equations in terms of a new variable $y(r)$ defined by

$$\delta p = y(r)Y_{\ell m}(\theta,\phi)e^{-i\omega t}. \tag{5.17}$$

As a consequence of Eq. (5.9) and the angular components of the perturbed Euler equation, we find that y is related to z by

$$y = \omega^2(\mu + p)z + (\mu - 3p)P. \tag{5.18}$$

Assuming that $\omega \neq 0$ (this special case will be considered below), the resulting equations can be manipulated to take the schematic form

$$0 = dx/dr + (\ )x + (\ )y + (\ )P, \tag{5.19a}$$

$$0 = dy/dr + (\ )x + (\ )y + (\ )P + (\ )dP/dr, \tag{5.19b}$$

$$0 = d^2P/dr^2 + (\ )dP/dr + (\ )x + (\ )y + (\ )P, \tag{5.19c}$$

where the various coefficients ( ) are functions of r constructed from the background fluid variables. The explicit form of these coefficients will be displayed below for the case of the modified $n = 1$ polytrope discussed in Sec. IV. For now, it suffices to notice that an analysis of Eqs. (5.19) near $r = 0$ reveals that when $\ell \neq 0$, the variables possess the asymptotic behavior

$$x \sim x_0 r^{\ell-1}, \qquad y \sim y_0 r^{\ell}, \qquad P \sim P_0 r^{\ell}, \tag{5.20}$$

where x_0 and P_0 are freely specifiable constants, and $\ell y_0 = \omega^2(\mu_c + p_c)x_0 + \ell(\mu_c - 3p_c)P_0$, with $\mu_c = \mu(r = 0)$, $p_c = p(r = 0)$. When $\ell = 0$ we have instead

$$x \sim x_1 r, \qquad y \sim y_0, \qquad P \sim P_0 + P_2 r^2, \tag{5.21}$$

where x_1 and P_0 are freely specifiable, while y_0 and P_2 can be expressed in terms of them.

The boundary conditions at $r = R$ are determined by $\Delta p = 0$, which identifies the true position of the surface, and the requirement that $\delta\Phi$ be smoothly joined with the external solution. The first equation gives $\delta p + \xi_r dp/dr = 0$, or $y - m(\mu - 3p)x/r^2 = 0$. Assuming that the background density μ goes to zero on the boundary, we find that

$$y(r = R) = 0. \tag{5.22}$$

Outside the body, the differential equation satisfied by P becomes

$$\frac{d^2P}{dr^2} + \frac{2}{r}\frac{dP}{dr} + \left[\omega^2 - \frac{\ell(\ell+1)}{r^2}\right]P = 0. \tag{5.23}$$

This is the spherical Bessel equation, and the solution describing an outgoing wave is

$$P_{\rm ext} = A h_\ell^{(1)}(\omega r), \tag{5.24}$$

where A is a constant amplitude and $h_\ell^{(1)} = j_\ell + iy_\ell$ is a spherical Hankel function. Equations (5.22) and (5.24) provide the required boundary conditions at $r = R$.

C. Modified $n = 1$ polytrope

For concreteness we now choose the unperturbed configuration to be the modified $n = 1$ polytrope described in Sec. IV. For simplicity we set

$$\Gamma_1 = 2, \qquad \Gamma_3 - 1 = 0. \tag{5.25}$$

The constant value for Γ_1 is a crude approximation that is entirely sufficient for our purposes. The exact expression, assuming that the perturbed fluid possesses the same equation of state as the unperturbed configuration, can be obtained from Eq. (4.5), and the approximation $\Gamma_1 \simeq 2$ is accurate when $M/R \ll 1$. We note that $\Gamma < \Gamma_1$ everywhere within the body, which suggests that it is locally stable against convection (see Sec. 9.3 of Ref. [41]).

The explicit system of perturbation equations for this model is as follows. We first introduce dimensionless variables $\bar r := r/R$, $\chi := M/R$, and $w := \omega\sqrt{R^3/M}$. When $\ell \neq 0$ we introduce new dimensionless variables e_j such that

$$x = R\bar r^{\ell-1} e_1, \qquad y = \chi^2 R^{-2}\bar r^{\ell} e_2, \qquad P = \chi \bar r^{\ell} e_3, \qquad \frac{dP}{dr} = \chi R^{-1}\bar r^{\ell-1} e_4, \tag{5.26}$$

and express the differential equations in the form

$$0 = \mathcal{E}_j := \bar r \frac{de_j}{d\bar r} + \mathcal{A}_j{}^k e_k, \tag{5.27}$$

where summation over the repeated index k is understood. The nonvanishing components of the matrix $\mathcal{A}_j{}^k$ are given by

$$\mathcal{A}_1{}^1 = \ell + \frac{\pi\bar r\cos\pi\bar r}{\sin\pi\bar r}, \tag{5.28a}$$

$$\mathcal{A}_1{}^2 = -\frac{4\pi\bar{r}^2\left\{\left[\ell(\ell+1)-2\chi(w\bar{r})^2\right]\sin\pi\bar{r}-\pi w^2\bar{r}^3\right\}}{w^2(\pi\bar{r}+2\chi\sin\pi\bar{r})\sin^2\pi\bar{r}}, \tag{5.28b}$$

$$\mathcal{A}_1{}^3 = \frac{\ell(\ell+1)\pi\bar{r}}{w^2(\pi\bar{r}+2\chi\sin\pi\bar{r})}, \tag{5.28c}$$

$$\mathcal{A}_2{}^1 = \frac{\chi}{2\pi^2\bar{r}^5}\sin^3\pi\bar{r} - \chi\left(\frac{w^2}{2\pi\bar{r}^2}+\frac{\cos\pi\bar{r}}{\pi\bar{r}^4}\right)\sin^2\pi\bar{r} - \left(\frac{w^2}{4\bar{r}}-\frac{\chi\cos^2\pi\bar{r}}{2\bar{r}^3}\right)\sin\pi\bar{r}, \tag{5.28d}$$

$$\mathcal{A}_2{}^2 = \ell+1+\chi\cos\pi\bar{r}-\frac{\chi\sin\pi\bar{r}}{\pi\bar{r}}-\frac{\pi\bar{r}\cos\pi\bar{r}}{\sin\pi\bar{r}}, \tag{5.28e}$$

$$\mathcal{A}_2{}^3 = -\frac{\chi\sin^2\pi\bar{r}}{4\pi\bar{r}^2}+\frac{\chi\sin\pi\bar{r}\cos\pi\bar{r}}{4\bar{r}}, \tag{5.28f}$$

$$\mathcal{A}_2{}^4 = -\frac{\sin\pi\bar{r}}{4\bar{r}}, \tag{5.28g}$$

$$\mathcal{A}_3{}^3 = \ell, \tag{5.28h}$$

$$\mathcal{A}_3{}^4 = -1, \tag{5.28i}$$

$$\mathcal{A}_4{}^1 = \frac{2\chi\sin^2\pi\bar{r}}{\bar{r}^2}-\frac{2\pi\chi\sin\pi\bar{r}\cos\pi\bar{r}}{\bar{r}}, \tag{5.28j}$$

$$\mathcal{A}_4{}^2 = \frac{4\pi^2\bar{r}^3}{\sin\pi\bar{r}}-4\pi\chi\bar{r}^2, \tag{5.28k}$$

$$\mathcal{A}_4{}^3 = -\ell(\ell+1)+\chi(w\bar{r})^2-\chi\pi\bar{r}\sin\pi\bar{r}, \tag{5.28l}$$

$$\mathcal{A}_4{}^4 = \ell+1. \tag{5.28m}$$

The variables admit the expansions

$$e_j = u_{j0}+u_{j2}\bar{r}^2+u_{j4}\bar{r}^4+\cdots \tag{5.29}$$

near $\bar{r}=0$. Analysis of Eqs. (5.27) around the origin reveals that of all the expansion coefficients in Eq. (5.29), $e_1(\bar{r}=0)=u_{10}$ and $e_3(\bar{r}=0)=u_{30}$ are freely-specifiable, and the remaining ones are determined in terms of them by the differential equations. In particular, regularity considerations imply that

$$e_2(\bar{r}=0)=u_{20}=\frac{\pi\omega^2}{4\ell}(1+2\chi)u_{10}+\frac{\pi}{4}u_{30}, \qquad e_4(\bar{r}=0)=u_{40}=\ell u_{30}. \tag{5.30}$$

Near $\bar{r}=1$ we have instead

$$e_j = v_{j0}+v_{j1}(\bar{r}-1)+v_{j2}(\bar{r}-1)^2+v_{j3}(\bar{r}-1)^3+\cdots. \tag{5.31}$$

The boundary condition (5.22) and the requirement that P be smoothly joined with the external solution (5.24) imply

$$e_2(\bar{r}=1)=v_{20}=0, \qquad e_4(\bar{r}=1)=v_{40}=\omega R\frac{h_\ell^{(1)\prime}(\omega R)}{h_\ell^{(1)}(\omega R)}v_{30} \tag{5.32}$$

where a prime indicates differentiation with respect to the argument. Thus, at $\bar{r}=1$ there are two freely specifiable constants, v_{10} and v_{30}, and the remaining coefficients are determined by the differential equations and by the boundary conditions (5.32).

When $\ell=0$ the new variables e_j are defined by

$$x = R\bar{r}e_1, \qquad y=\chi^2R^{-2}e_2, \qquad P=\chi e_3, \qquad \frac{dP}{dr}=\chi R^{-1}\bar{r}e_4, \tag{5.33}$$

and the differential equations are again put in the form of Eq. (5.27). In this case the nonvanishing components of $\mathcal{A}_j{}^k$ are given by

$$\mathcal{A}_1{}^1 = 2+\frac{\pi\bar{r}\cos\pi\bar{r}}{\sin\pi\bar{r}}, \tag{5.34a}$$

$$\mathcal{A}_1{}^2 = \frac{4\pi\bar{r}^2}{\sin^2\pi\bar{r}}, \tag{5.34b}$$

$$\mathcal{A}_2{}^1 = \frac{\chi}{2\pi^2\bar{r}^3}\,\sin^3\pi\bar{r} - \chi\left(\frac{w^2}{2\pi} + \frac{\cos\pi\bar{r}}{\pi\bar{r}^2}\right)\sin^2\pi\bar{r} - \left(\frac{w^2\bar{r}}{4} - \frac{\chi\cos^2\pi\bar{r}}{2\bar{r}}\right)\sin\pi\bar{r}, \tag{5.34c}$$

$$\mathcal{A}_2{}^2 = 1 + \chi\cos\pi\bar{r} - \frac{\chi\sin\pi\bar{r}}{\pi\bar{r}} - \frac{\pi\bar{r}\cos\pi\bar{r}}{\sin\pi\bar{r}}, \tag{5.34d}$$

$$\mathcal{A}_2{}^3 = -\frac{\chi\sin^2\pi\bar{r}}{4\pi\bar{r}^2} + \frac{\chi\sin\pi\bar{r}\cos\pi\bar{r}}{4\bar{r}}, \tag{5.34e}$$

$$\mathcal{A}_2{}^4 = -\frac{1}{4}\bar{r}\sin\pi\bar{r}, \tag{5.34f}$$

$$\mathcal{A}_3{}^4 = -\bar{r}^2, \tag{5.34g}$$

$$\mathcal{A}_4{}^1 = \frac{2\chi\sin^2\pi\bar{r}}{\bar{r}^2} - \frac{2\pi\chi\sin\pi\bar{r}\cos\pi\bar{r}}{\bar{r}}, \tag{5.34h}$$

$$\mathcal{A}_4{}^2 = \frac{4\pi^2\bar{r}}{\sin\pi\bar{r}} - 4\pi\chi, \tag{5.34i}$$

$$\mathcal{A}_4{}^3 = \chi w^2 - \frac{\pi M}{\bar{r}}\sin\pi\bar{r}, \tag{5.34j}$$

$$\mathcal{A}_4{}^4 = 3. \tag{5.34k}$$

In this case also the variables admit the expansions of Eqs. (5.29) and (5.31), with u_{10}, u_{30}, v_{10}, and v_{30} freely specifiable and the remaining coefficients determined by the differential equations and by the boundary conditions (5.32) with $\ell = 0$.

D. Eigenfrequencies and quasinormal modes

Equations (5.27) form a fourth-order system of differential equations. In principle, the set of regularity and boundary conditions given in Eqs. (5.30) and (5.32) provides the required data to close the system. However, since Eqs. (5.27) are linear and homogeneous, the functions e_j are determined only up to a multiplicative constant; this implies that the system will have no solution unless ω is chosen appropriately. The system is therefore an eigenvalue problem for ω. Because $P_{\rm ext}$ is necessarily a complex function, the solution to the eigenvalue problem is a set of complex frequencies $\omega := \sigma - i\kappa$,where σ and κ are both real.

The eigenfrequencies are determined as follows. The differential equations (5.27) for $e_j(r)$ are first integrated outward from $\bar{r} = 0$, together with (5.30), and with u_{10} chosen arbitrarily to provide a normalization for the solution. Next the differential equations are integrated inward from $\bar{r} = 1$, together with Eq. (5.32). There are four freely specifiable complex constants, $\{\omega, u_{30}, v_{10}, v_{30}\}$ or $\{\omega, u_{30}, v_{10}, A\}$, and these are adjusted so that at a point $\bar{r} = r_1$ such that $0 < r_1 < 1$, the functions $e_j^{\rm out}(r)$, integrated outward from $\bar{r} = 0$, match the functions $e_j^{\rm in}(r)$, integrated inward from $\bar{r} = 1$: this provides a set of four (complex) conditions to be solved for the four unknown constants. The search for the solution is performed with a globally convergent version of the Newton-Raphson method, as described in Sec. 9.7 of Ref. [42]. The numerical computation of high overtones (i.e., with large values of $|n|$; see below) is particularly challenging, since $|{\rm Im}(\omega)|$ decays exponentially with increasing $|n|$, as does the constant A. An increasingly high resolution is required in order to compute them, and we find that floating-point operations with double precision are not always enough to achieve convergence. We overcome this technical issue by computing these high overtones in both *Mathematica* and *Maple*, in which a higher numerical precision can be easily stipulated.

Once a solution is found for σ (the mode frequency) and κ (the inverse of the damping time), the perturbation equations can be integrated once more to obtain the perturbation variables $\xi_r = x(r)Y_{\ell m}(\theta,\phi)e^{-\kappa t}e^{i\sigma t}$, $\delta p = y(r)Y_{\ell m}(\theta,\phi)e^{-\kappa t}e^{i\sigma t}$, and $\delta\Phi = P(r)Y_{\ell m}(\theta,\phi)e^{-\kappa t}e^{i\sigma t}$ throughout the fluid; these describe the quasinormal modes of the body. For each ℓ the modes are characterized by the number n of nodes in $x(r)$ or $y(r)$. The mode with $n = 0$ is the *fundamental mode* (f-mode), and modes with $n > 0$ divide themselves into *pressure modes* (p-modes) and *gravity modes* (g-modes). The frequencies of the p-modes are higher than the f-mode frequency, and they increase with the mode number n. On the other hand, the frequencies of the g-modes are lower than the f-mode frequency, and they decrease with increasing $|n|$. It is conventional to assign a negative value of n to the g-modes, and we adopt this practice here.

The result of our computations for a fluid body with $\chi = 0.3$ were already presented in Fig. 1, and another perspective is offered in Fig. 7. It was pointed out that many of the quasinormal modes, in particular the g-modes, have extremely small values of κ, which makes them extremely long-lived. It is also noteworthy that a number of p-modes are in fact unstable, with $\kappa < 0$. These unstable modes, however, have virtually no impact on the self-force results presented in Sec. VI.

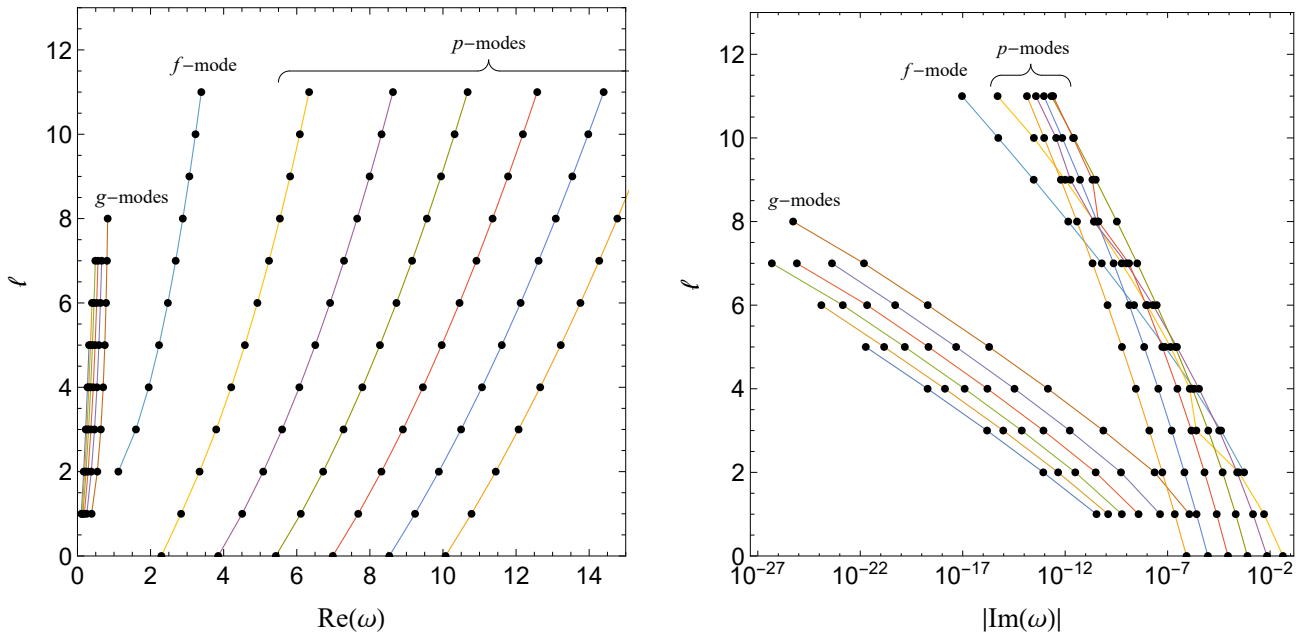

FIG. 7. Real and (modulus of the) imaginary parts of the quasinormal-mode frequencies ω of a fluid body with compactness $M/R = 0.3$ in the scalar theory of gravity, for the lower multipole orders. Frequencies are presented in units of $\sqrt{M/R^3}$. The mode frequencies are grouped in families of definite mode number n, and classified as g-, f- or p-modes as described in the main text.

E. Static perturbations

The case $\omega = 0$ requires a separate treatment. In this case the manipulations leading to the system of equations (5.19) break down, because as Eq. (5.18) indicates, y is no longer independent from P. A further study of the perturbation equations also reveals that $x = (r^2/m)P$, and that z can be expressed in terms of P and its first derivative. The entire content of the perturbation equations is therefore summarized in the equation for P, which becomes

$$r^2\frac{d^2P}{dr^2} + 2r\frac{dP}{dr} - \left[12\pi r^2(\mu - 3p) + \frac{4\pi r^4}{m}\frac{d\mu}{dr} + \ell(\ell+1)\right]P = 0. \tag{5.35}$$

When the unperturbed configuration is that of a modified $n = 1$ polytrope, the differential equation becomes

$$r^2\frac{d^2P}{dr^2} + 2r\frac{dP}{dr} + \left[(\pi r/R)^2 - \ell(\ell+1)\right]P = 0. \tag{5.36}$$

This is the spherical Bessel equation, with solution

$$P = Bj_\ell(\pi r/R), \tag{5.37}$$

where B is an arbitrary amplitude.

VI. SCALAR GRAVITY WITH FLUID BODY AND POINT PARTICLE

In this section we generalize the foregoing discussion by allowing the system to also include a point particle, which is assumed to move outside the fluid body on a world line described by the parametric relations $z^\alpha(s)$, where s is proper time on the world line. We continue to set $\alpha(\Phi) = 1$ and to take the spacetime metric to be flat.

A. Defining equations

The insertion of the point particle is accomplished by generalizing the field equations to

$$\Box\Phi = 4\pi\big(T^{\mu}_{\ \mu} + \mathfrak{t}^{\mu}_{\ \mu}\big), \qquad \nabla_\beta\big(T^{\alpha\beta} + \mathfrak{t}^{\alpha\beta}\big) = -\big(T^{\mu}_{\ \mu} + \mathfrak{t}^{\mu}_{\ \mu}\big)\nabla^\alpha\Phi, \tag{6.1}$$

where $T^{\alpha\beta}$ continues to denote the fluid's energy-momentum tensor, while

$$\mathfrak{t}^{\alpha\beta} = \int \mathfrak{m}\, v^\alpha v^\beta \delta_4(x,z)\, ds \tag{6.2}$$

is the energy-momentum tensor of the particle, with $\mathfrak{m}(s)$ denoting its (time-dependent) mass, $v^\alpha = dz^\alpha/ds$ its velocity vector, and $\delta_4(x,z)$ a scalarized Dirac delta-function supported on the particle's world line — x stands for an arbitrary spacetime point, while $z(s)$ is a point on the world line. By virtue of the assumption that the particle moves outside the fluid distribution, the supports of $T^{\alpha\beta}$ and $\mathfrak{t}^{\alpha\beta}$ are disjoint, and the equations of motion decompose into a conservation equation for the fluid alone,

$$\nabla_\beta T^{\alpha\beta} = -T^{\mu}_{\ \mu}\,\nabla^\alpha\Phi, \tag{6.3}$$

and a conservation equation for the particle alone,

$$\nabla_\beta \mathfrak{t}^{\alpha\beta} = -\mathfrak{t}^{\mu}_{\ \mu}\,\nabla^\alpha\Phi. \tag{6.4}$$

The first equation produces the same fluid equations that were studied in the preceding sections. The second equation implies

$$\frac{D}{ds}\big(\mathfrak{m}v^\alpha\big) = \mathfrak{m}\nabla^\alpha\Phi(z), \tag{6.5}$$

which can be decomposed into

$$\frac{d\mathfrak{m}}{ds} = -\mathfrak{m}v^\alpha\nabla_\alpha\Phi(z), \qquad \frac{Dv^\alpha}{ds} = \big(\eta^{\alpha\beta} + v^\alpha v^\beta\big)\nabla_\beta\Phi(z). \tag{6.6}$$

The particle and the fluid are coupled through the potential Φ, which now satisfies the wave equation

$$\Box\Phi = -4\pi(\mu - 3p) - 4\pi\int \mathfrak{m}\,\delta_4(x,z)\, ds. \tag{6.7}$$

In the body's interior the second term vanishes, and the wave equation reduces to the one studied in the preceding sections. In the exterior the first term vanishes, and Φ is sourced by the particle only.

We observe that the insertion of the particle has no impact on the fluid equations, which are identical to those considered previously. The particle nevertheless influences the fluid's dynamics through the boundary values adopted by Φ, which are now different from those considered previously. The particle is also affected by the fluid, through the same boundary conditions. The motion of the fluid and the motion of the particle are inherently coupled.

B. Unperturbed and perturbed configurations

As in Sec. V we take the unperturbed configuration of the system to be a spherically-symmetric distribution of fluid in hydrostatic equilibrium, in the absence of a point particle. This configuration is described by the unperturbed variables μ, p, u^α, and Φ; outside the body $\Phi = M/r$. The insertion of the particle creates a perturbed configuration, and the perturbation is described by the variables $\Delta\mu$, Δp, Δu^α, $\delta\Phi$, $\mathfrak{m}$, and v^α.

As we observed at the end of the preceding subsection, the equations for the fluid perturbations take the same form as those studied previously. On the other hand, the equation for $\delta\Phi$ becomes

$$\Box\delta\Phi = -4\pi(\delta\mu - 3\delta p) - 4\pi\int \mathfrak{m}\,\delta_4(x,z)\, ds, \tag{6.8}$$

which reduces to Eq. (5.14) inside the body, and to

$$\Box\delta\Phi_{\rm out} = -4\pi\int \mathfrak{m}\,\delta_4(x,z)\, ds \tag{6.9}$$

outside the body. The particle's variables are determined by

$$\frac{d\mathfrak{m}}{ds} = -\mathfrak{m}v^\alpha\nabla_\alpha\Phi - \mathfrak{m}v^\alpha\nabla_\alpha\delta\Phi_{\rm out} \tag{6.10}$$

and

$$\frac{Dv^\alpha}{ds} = \big(\eta^{\alpha\beta} + v^\alpha v^\beta\big)\nabla_\beta\Phi + \big(\eta^{\alpha\beta} + v^\alpha v^\beta\big)\nabla_\beta\delta\Phi_{\rm out}, \tag{6.11}$$

with the first set of terms representing the particle's motion in the background potential Φ, and the second set representing the self-force.

We take the motion of the particle in the background potential $\Phi = M/r$ to be a circular orbit of radius $r = r_0$ and angular velocity Ω in the equatorial plane ($\theta = \pi/2$) of the fluid body. A simple calculation reveals that in the coordinates (t, r, θ, ϕ), the components of the velocity vector are given by

$$v^\alpha = \gamma(1, 0, 0, \Omega), \qquad \gamma = \sqrt{1 + M/r_0}, \qquad \Omega^2 = \frac{M/r_0^3}{1 + M/r_0}. \tag{6.12}$$

Because $v^\alpha\nabla_\alpha\Phi = 0$, the particle's mass $\mathfrak{m}$ is conserved in the background motion.

The particle creates the perturbation $\delta\Phi_{\rm out}$, and for the circular orbit the source term of Eq. (6.9) can be written as

$$\begin{aligned} 4\pi\int \mathfrak{m}\,\delta_4(x, z)\,ds &= \frac{4\pi\mathfrak{m}}{\gamma r_0^2}\delta(r - r_0)\delta(\theta - \pi/2)\delta(\phi - \Omega t) \\ &= \frac{4\pi\mathfrak{m}}{\gamma r_0^2}\delta(r - r_0)\sum_{\ell m} Y^*_{\ell m}(\pi/2, \Omega t)Y_{\ell m}(\theta, \phi) \\ &= \frac{4\pi\mathfrak{m}}{\gamma r_0^2}\delta(r - r_0)\sum_{\ell m} e^{-im\Omega t}Y_{\ell m}(\pi/2, 0)Y_{\ell m}(\theta, \phi), \end{aligned} \tag{6.13}$$

where an asterisk indicates complex conjugation, and the sums over ℓ and m run from 0 to ∞ and from $-\ell$ to ℓ, respectively.

The preceding expression indicates that the mass density has a frequency spectrum limited to harmonics of the orbital frequency Ω. It implies that $\delta\Phi_{\rm out}$ can be expanded as

$$\delta\Phi_{\rm out} = \sum_{\ell m} P_{\ell m}(r)Y_{\ell m}(\theta, \phi)e^{-im\Omega t}, \tag{6.14}$$

with the radial functions $P_{\ell m}(r)$ determined by Eq. (6.9). The radial equation takes the form of

$$\frac{d^2P_{\ell m}}{dr^2} + \frac{2}{r}\frac{dP_{\ell m}}{dr} + \left[\omega^2 - \frac{\ell(\ell + 1)}{r^2}\right]P_{\ell m} = -\frac{G_{\ell m}}{r_0^2}\delta(r - r_0), \tag{6.15}$$

where $\omega = m\Omega$ and

$$G_{\ell m} := \frac{4\pi\mathfrak{m}}{\gamma}Y_{\ell m}(\pi/2, 0). \tag{6.16}$$

It should be noted that the sum over m in Eq. (6.14) is restricted to values such that $\ell + m$ is even, because $Y_{\ell m}(\pi/2, 0)$ vanishes when $\ell + m$ is odd. For $\ell + m$ even we have instead

$$Y_{\ell m}(\pi/2, 0) = (-1)^{\frac{1}{2}(\ell+m)}\sqrt{\frac{2\ell + 1}{4\pi}}\frac{\sqrt{(\ell - m)!(\ell + m)!}}{(\ell - m)!!(\ell + m)!!}. \tag{6.17}$$

It should also be noted that $\delta\Phi_{\rm out}$ is real when $P_{\ell m}$ satisfies the conditions

$$P_{\ell,-m} = (-1)^m P^*_{\ell m}. \tag{6.18}$$

These conditions have to be respected when boundary conditions are adopted for the radial functions.

C. Solution to the perturbation equations ($m \neq 0$)

We now construct the appropriate solutions to Eq. (6.15) and the remaining perturbation equations, assuming first that $m \neq 0$, so that $\omega = m\Omega$ is nonzero. When $r \neq r_0$ the differential equation reduces to the spherical Bessel equation, with $j_\ell(\omega r)$ and $y_\ell(\omega r)$ as linearly independent solutions. When $r > r_0$ the solution must represent an outgoing wave, and to reflect this we write

$$P^{>}_{\ell m} = \omega G_{\ell m} A_\ell(\omega)\big[j_\ell(\omega r) + i y_\ell(\omega r)\big], \tag{6.19}$$

where $A_\ell(\omega)$ is a complex amplitude and a factor of $\omega G_{\ell m}$ was inserted for convenience. For $r < r_0$ we have instead

$$P^{<}_{\ell m} = \omega G_{\ell m}\big[B_\ell(\omega) j_\ell(\omega r) + C_\ell(\omega) y_\ell(\omega r)\big], \tag{6.20}$$

where $B_\ell(\omega)$ and $C_\ell(\omega)$ can be related to $A_\ell(\omega)$ by the junction conditions implied by the presence of a delta-function on the right-hand side of Eq. (6.15). A simple calculation returns

$$B_\ell(\omega) = A_\ell(\omega) - y_\ell(\omega r_0), \qquad C_\ell(\omega) = i A_\ell(\omega) + j_\ell(\omega r_0); \tag{6.21}$$

the end result was simplified by exploiting the Wronskian relation $j_\ell y'_\ell - j'_\ell y_\ell = (\omega r)^{-2}$ satisfied by the spherical Bessel functions, with a prime indicating differentiation with respect to the argument ωr.

The function $P^{<}_{\ell m}(r)$ must be matched to a solution of the fluid perturbation equations (5.27) at the body's boundary, situated at $r = R$. With ω now real, these fluid perturbation equations admit real solutions. We take advantage of this property through the following procedure. Ignoring for the moment the boundary condition coming from the matching to the external potential, we have five freely specifiable constants: $\{u_{10}, u_{30}, v_{10}, v_{30}, v_{40}\}$, corresponding to $\{e_1(r=0), e_3(r=0), e_1(r=R), e_3(r=R), e_4(r=R)\}$. If we fix the normalization by setting, e.g., $v_{10} = 1$, then the four remaining constants can be determining by adapting the method described in Sec. V D to find the quasinormal modes of the fluid distribution. The system of equations (5.27) is integrated outward from $r = 0$ with unknown boundary values u_{10} and u_{30}, and it is integrated inward from $r = R$ with unknown boundary values v_{30} and v_{40}. We then determine the four unknown constants by imposing continuity of $e_j(r)$ at a middle point $r = r_1$. Let us call the solution thus obtained $\hat{e}_j(r)$. Then, the actual complex solution, that matches $P^{<}_{\ell m}(r)$ at $r = R$, can be obtained from $\hat{e}_j(r)$ by a simple (complex) rescaling: $e_j(r) = N_\ell(\omega)\hat{e}_j(r)$. Recalling the definitions of Eq. (5.26), we have that the matching conditions at $r = R$ are

$$\chi N_\ell(\omega)\hat{e}_3(R) = P^{<}_{\ell m}(r=R) = \omega G_{\ell m}\Big\{\big[A_\ell(\omega) - y_\ell(\omega r_0)\big] j_\ell(\omega R) + \big[i A_\ell(\omega) + j_\ell(\omega r_0)\big] y_\ell(\omega R)\Big\}, \tag{6.22a}$$

$$R^{-1}\chi N_\ell(\omega)\hat{e}_4(R) = \frac{dP^{<}_{\ell m}}{dr}(r=R) = \omega^2 G_{\ell m}\Big\{\big[A_\ell(\omega) - y_\ell(\omega r_0)\big] j'_\ell(\omega R) + \big[i A_\ell(\omega) + j_\ell(\omega r_0)\big] y'_\ell(\omega R)\Big\}. \tag{6.22b}$$

These equations determine $A_\ell(\omega)$ and $N_\ell(\omega)$ in terms of the known amplitudes $\hat{e}_3(R)$ and $\hat{e}_4(R)$. Writing

$$A_\ell(\omega) = \alpha_\ell(\omega) + i\beta_\ell(\omega), \tag{6.23}$$

we find that

$$\alpha_\ell(\omega) = \frac{\big[R\omega(y_0 j' - j_0 y')\hat{e}_3 + (j_0 y - y_0 j)\hat{e}_4\big](R\omega j'\hat{e}_3 - j\hat{e}_4)}{R^2\omega^2(j'^2 + y'^2)\hat{e}_3^2 - 2R\omega(y'y + j'j)\hat{e}_3\hat{e}_4 + (j^2 + y^2)\hat{e}_4^2}, \tag{6.24a}$$

$$\beta_\ell(\omega) = -\frac{\big[R\omega(y_0 j' - j_0 y')\hat{e}_3 + (j_0 y - y_0 j)\hat{e}_4\big](R\omega y'\hat{e}_3 - y\hat{e}_4)}{R^2\omega^2(j'^2 + y'^2)\hat{e}_3^2 - 2R\omega(y'y + j'j)\hat{e}_3\hat{e}_4 + (j^2 + y^2)\hat{e}_4^2}, \tag{6.24b}$$

where $\hat{e}_3 := \hat{e}_3(R)$, $\hat{e}_4 := \hat{e}_4(R)$, $j_0 := j_\ell(\omega r_0)$, $y_0 := y_\ell(\omega r_0)$, $j := j_\ell(\omega R)$, and $y := y_\ell(\omega R)$.

D. Solution to the perturbation equations ($m = 0$)

We next turn to the special case $m = 0$, which implies $\omega = 0$. In this case the linearly independent solutions to Eq. (6.15) are r^ℓ and $r^{-(\ell+1)}$. The appropriate solution for $r > r_0$ is

$$P^{>}_{\ell 0} = \frac{Z_\ell}{2\ell + 1}\frac{G_{\ell 0}}{r_0}(r_0/r)^{\ell+1}, \tag{6.25}$$

where Z_ℓ is a real amplitude. The junction conditions at $r = r_0$ imply that

$$P^<_{\ell 0} = \frac{1}{2\ell+1}\frac{G_{\ell 0}}{r_0}\Big[(r/r_0)^\ell + (Z_\ell - 1)(r_0/r)^{\ell+1}\Big] \tag{6.26}$$

is the correct solution for $r < r_0$.

The function $P^<_{\ell 0}$ must be matched to the internal solution of Eq. (5.37) at the boundary $r = R$, and the procedure returns

$$Z_\ell - 1 = \frac{1}{\bar{r}_0^{2\ell+1}}\frac{\ell j_\ell(\pi) - \pi j'_\ell(\pi)}{(\ell+1)j_\ell(\pi) + \pi j'_\ell(\pi)}, \tag{6.27}$$

where $\bar{r}_0 := r_0/R$.

When $\ell = 0$ the function $P^<_{00}$ must be constant, because a term proportional to r^{-1} would represent an unphysical shift in the body's mass. Removing this term amounts to setting $Z_0 = 1$, and we obtain

$$P^>_{00} = \frac{G_{00}}{r}, \qquad P^<_{00} = \frac{G_{00}}{r_0}. \tag{6.28}$$

With $G_{00} = \sqrt{4\pi}\mathfrak{m}/\gamma$, we find that the $\ell = m = 0$ contribution to $\delta\Phi_{\rm out}$ is given by $\mathfrak{m}/(\gamma r)$ when $r > r_0$, which indicates that $\mathfrak{m}/\gamma$ is the particle's gravitational mass. The fact that P_{00} is constant when $r < r_0$ implies that the $\ell = m = 0$ mode of the perturbation vanishes inside the body.

E. Solution to the perturbation equations in the absence of a star

For the eventual purpose of regularizing the mode sum for the self-force, we examine once more a particle of mass $\mathfrak{m}$ on a circular orbit of radius r_0 and angular velocity Ω, but this time in the absence of a fluid body. (In this case the particle is maintained on its orbit by an external agent instead of the body's gravitational field.) The solutions to Eq. (6.15) are unchanged for $r > r_0$, but the solutions for $r < r_0$ must now be nonsingular at $r = 0$.

When $m \neq 0$ the regularity condition implies that $C_\ell(\omega) = 0$, which produces

$$P^>_{\ell m} = i\omega G_{\ell m} j_\ell(\omega r_0) h^{(1)}_\ell(\omega r), \qquad P^<_{\ell m} = i\omega G_{\ell m} h^{(1)}_\ell(\omega r_0) j_\ell(\omega r), \tag{6.29}$$

where $\omega = m\Omega$. When $m = 0$ the regularity condition implies that $Z_\ell = 1$, so that

$$P^>_{\ell 0} = \frac{1}{2\ell+1}\frac{G_{\ell 0}}{r_0}(r_0/r)^{\ell+1}, \qquad P^<_{\ell 0} = \frac{1}{2\ell+1}\frac{G_{\ell 0}}{r_0}(r/r_0)^{\ell}. \tag{6.30}$$

For $\ell = m = 0$ the solution is

$$P^>_{00} = \frac{G_{00}}{r}, \qquad P^<_{00} = \frac{G_{00}}{r_0}, \tag{6.31}$$

unchanged relative to the previous expressions.

F. Self-force

The self-force acting on the particle is described by the second set of terms in Eqs. (6.10) and (6.11),

$$\dot{\mathfrak{m}} := \frac{d\mathfrak{m}}{ds} = -\mathfrak{m} v^\alpha \nabla_\alpha \delta\Phi \tag{6.32}$$

and

$$\mathfrak{f}^\alpha := \mathfrak{m}\frac{Dv^\alpha}{ds} = \mathfrak{m}\big(\eta^{\alpha\beta} + v^\alpha v^\beta\big)\nabla_\beta \delta\Phi, \tag{6.33}$$

where v^α is the velocity vector of Eq. (6.12), and $\delta\Phi \equiv \delta\Phi_{\rm out}$ is the potential of Eq. (6.14), which in unbounded in the limit $x \to z(s)$, that is, when evaluated at the position of the particle, $r = r_0$, $\theta = \pi/2$, and $\phi = \Omega t$.

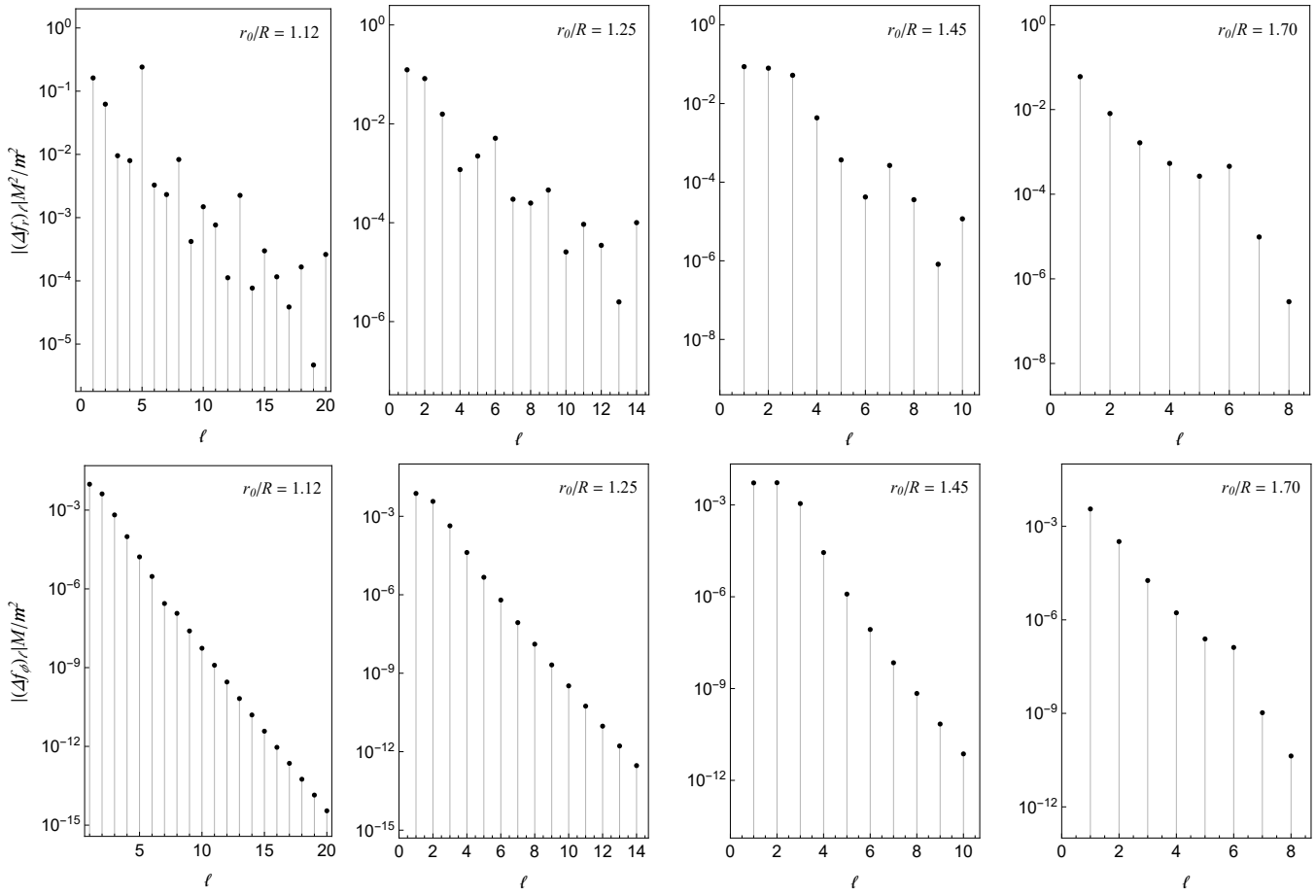

FIG. 8. In the upper panel the contributions of $(M^2/\mathfrak{m}^2)(\Delta \mathfrak{f}_r)_\ell$ from low multipole orders ℓ are shown, for selected values of r_0/R; for each one, the sum from $m = -\ell$ to ℓ was evaluated. As a general rule, to achieve a specified degree of accuracy (say 10^{-5}), the sum over ℓ must be truncated at a larger value when r_0/R is smaller. The rule is complicated by the resonant features, which can make a given contribution abnormally large. The lower panel shows the contributions of $(M/\mathfrak{m}^2)(\Delta \mathfrak{f}_\phi)_\ell$ from low multipole orders ℓ, for the same values of r_0/R. Here the convergence of the mode sum is much faster, and is not strongly affected by the resonant features.

To regularize the expressions of Eqs. (6.32) and (6.33) we examine the *difference* between two self-forces [43], the first resulting in the presence of the fluid body, the other resulting in its absence; in both cases the particle moves on the same circular orbit of radius r_0 and angular velocity Ω. We introduce a potential $\delta\Phi^{\rm S}$ that corresponds to the absence of the body, and write the self-force difference as

$$\Delta \dot{\mathfrak{m}} = -\mathfrak{m} v^\alpha \nabla_\alpha \big(\delta\Phi - \delta\Phi^{\rm S}\big), \qquad \Delta \mathfrak{f}_\alpha = \mathfrak{m}\big(\delta_\alpha{}^\beta + v_\alpha v^\beta\big)\nabla_\beta\big(\delta\Phi - \delta\Phi^{\rm S}\big). \tag{6.34}$$

Because $\delta\Phi$ and $\delta\Phi^{\rm S}$ are sourced by the same particle on the same circular orbit, they are equally singular at the position of the particle; their difference satisfies a homogeneous wave equation and is smooth at $x = z(s)$. The actual self-force is then

$$\dot{\mathfrak{m}} = \Delta\dot{\mathfrak{m}} + \dot{\mathfrak{m}}^{\rm S}, \qquad \mathfrak{f}_\alpha = \Delta\mathfrak{f}_\alpha + \mathfrak{f}^{\rm S}_\alpha, \tag{6.35}$$

with the second terms representing the self-force acting on the particle in the absence of a fluid body. The equations governing $\delta\Phi^{\rm S}$ and the motion of the particle in this potential are strictly identical to those governing the motion of a (constant) scalar charge $q \equiv \mathfrak{m}$ coupled to a scalar potential in flat spacetime, and the resulting expression for the self-force is well known (see, for example, Sec. 17.6 of Ref. [25]). We have

$$\dot{\mathfrak{m}}^{\rm S} = 0, \qquad \mathfrak{f}^{\rm S}_\alpha = \frac{1}{3}\mathfrak{m}^2\big(\eta_{\alpha\beta} + v_\alpha v_\beta\big)\frac{D^2 v^\beta}{ds^2}. \tag{6.36}$$

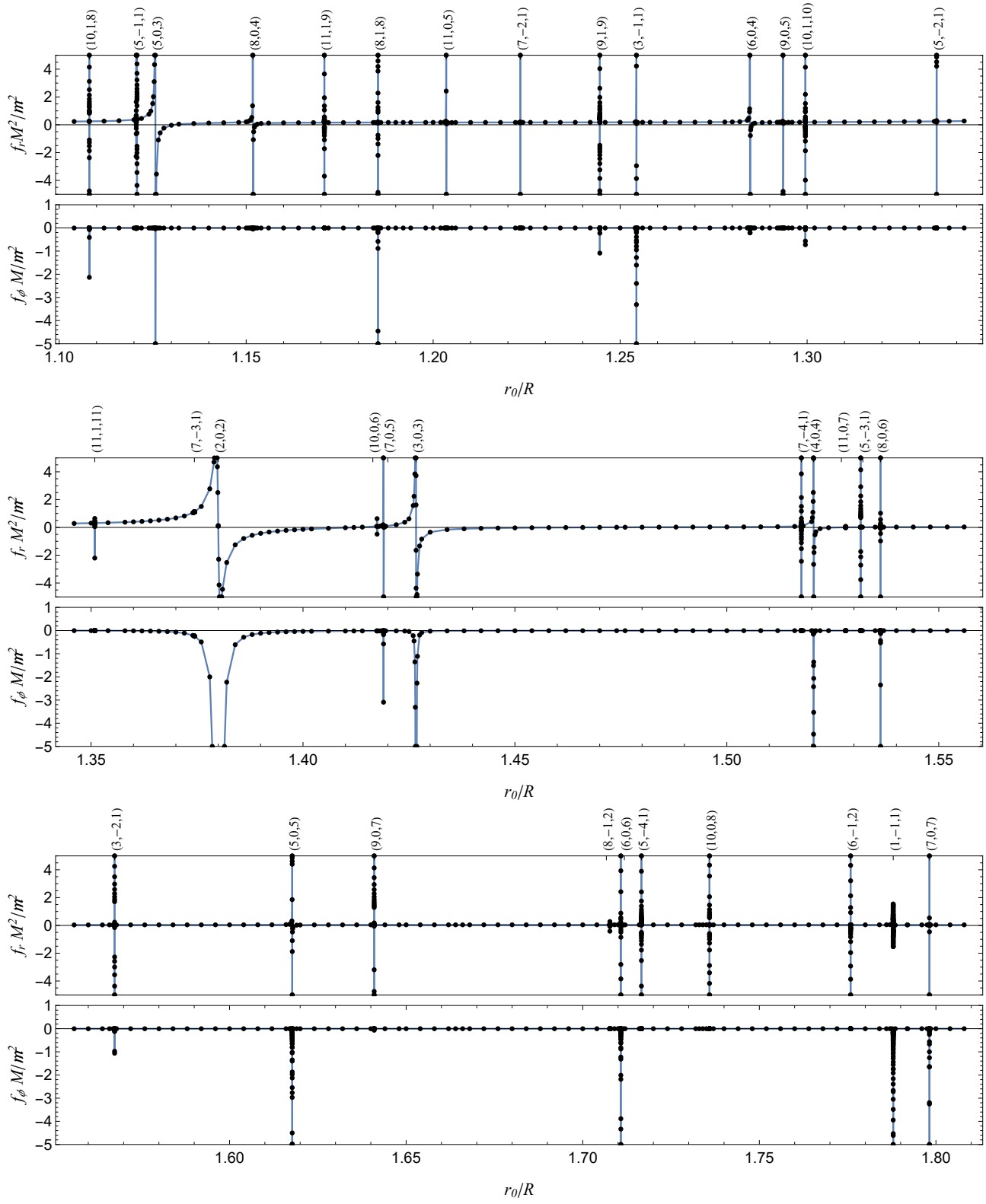

FIG. 9. Plots of $(M^2/\mathfrak{m}^2)\mathfrak{f}_r$ (upper panels) and $(M/\mathfrak{m}^2)\mathfrak{f}_\phi$ (lower panels) as functions of r_0/R in three successive subintervals of $1.10 < r_0/R < 1.81$. Each resonant feature in the self-force is associated with the relevant quasinormal mode, labeled by (ℓ, n, m). (The resonance identified by $(5, -1, 1)$ actually consists of two close resonant peaks, corresponding to $(5, -1, 1)$ and $(7, 1, 7)$.) Note that while quasinormal modes are independent of m, so that only ℓ and n are true mode labels, a resonance is achieved when $m\Omega = \mathrm{Re}(\omega)$, so that m is a required label for each resonance. Notice, in particular, the broad resonance near $r_0/M \simeq 1.38$, which is associated with the $\ell = 2$ f-mode ($n = 0$), and requires $m = 2$ for a frequency match.

The only nonvanishing components of $\mathfrak{f}^{\rm S}_\alpha$ are

$$\mathfrak{f}^{\rm S}_t = -\Omega\,\mathfrak{f}^{\rm S}_\phi, \qquad \mathfrak{f}^{\rm S}_\phi = -\frac{1}{3}\mathfrak{m}^2\frac{M^{3/2}}{r_0^{5/2}}(1+M/r_0) \tag{6.37}$$

for the circular orbit under consideration.

The self-force difference can be evaluated straightforwardly by means of a (convergent) mode sum. We write

$$\delta\Phi^{\rm S} = \sum_{\ell m} P^{\rm S}_{\ell m}(r) Y_{\ell m}(\theta,\phi) e^{-im\Omega t} \tag{6.38}$$

and let $\Delta P_{\ell m} := P_{\ell m} - P^{\rm S}_{\ell m}$. Inserting this and Eq. (6.14) into Eqs. (6.34) and evaluating at $r = r_0$, $\theta = \pi/2$, and $\phi = \Omega t$, we find after simple manipulations that

$$\Delta\dot{\mathfrak{m}} = 0, \tag{6.39a}$$
$$\Delta\mathfrak{f}_t = -\Omega\,\Delta\mathfrak{f}_\phi, \tag{6.39b}$$
$$\Delta\mathfrak{f}_r = \mathfrak{m}\sum_{\ell m}\frac{d}{dr}\Delta P_{\ell m}(r_0)\,Y_{\ell m}(\pi/2,0), \tag{6.39c}$$
$$\Delta\mathfrak{f}_\theta = 0, \tag{6.39d}$$
$$\Delta\mathfrak{f}_\phi = \mathfrak{m}\sum_{\ell m} im\Delta P_{\ell m}(r_0)\,Y_{\ell m}(\pi/2,0). \tag{6.39e}$$

Because $dP_{\ell m}/dr$ and $dP^{\rm S}_{\ell m}/dr$ are both discontinuous at $r = r_0$, they must be consistently evaluated either at $r = r_0^+$ or at $r = r_0^-$. The choice is immaterial, because the difference is continuous, but it is convenient to do the evaluation at $r = r_0^+$. The mode sums can be simplified by exploiting the reality conditions of Eq. (6.18). By folding the $m < 0$ part of the sum into the $m > 0$ part, we obtain

$$\Delta\mathfrak{f}_r = \mathfrak{m}\sum_\ell\biggl\{\frac{d}{dr}\Delta P_{\ell 0}(r_0^+)\,Y_{\ell 0}(\pi/2,0) + 2\sum_{m>0}\mathrm{Re}\biggl[\frac{d}{dr}\Delta P_{\ell m}(r_0)\biggr]Y_{\ell m}(\pi/2,0)\biggr\}, \tag{6.40a}$$
$$\Delta\mathfrak{f}_\phi = -2\mathfrak{m}\sum_\ell\sum_{m>0} m\,\mathrm{Im}\Bigl[\Delta P_{\ell m}(r_0)\Bigr]Y_{\ell m}(\pi/2,0). \tag{6.40b}$$

For the final expressions we import the results obtained in Secs. VI C, VI D, and VI E for the radial functions. After some simple algebra we find that the self-force differences are given by

$$\Delta\dot{\mathfrak{m}} = 0, \qquad \Delta\mathfrak{f}_t = -\Omega\,\Delta\mathfrak{f}_\phi, \qquad \Delta\mathfrak{f}_r = \sum_{\ell=1}^\infty\bigl(\Delta\mathfrak{f}_r\bigr)_\ell, \qquad \Delta\mathfrak{f}_\theta = 0, \qquad \Delta\mathfrak{f}_\phi = \sum_{\ell=1}^\infty\bigl(\Delta\mathfrak{f}_\phi\bigr)_\ell, \tag{6.41}$$

with

$$\begin{aligned}\bigl(\Delta\mathfrak{f}_r\bigr)_\ell = &-\frac{\ell+1}{2\ell+1}\mathfrak{m}G_{\ell 0}Y_{\ell 0}(\pi/2,0)\frac{Z_\ell - 1}{r_0^2}\\ &+ 2\sum_{m>0}^{\ell}\mathfrak{m}G_{\ell m}Y_{\ell m}(\pi/2,0)\,\omega^2\Bigl\{\alpha_\ell(\omega)j'_\ell(\omega r_0) - \bigl[\beta_\ell(\omega) - j_\ell(\omega r_0)\bigr]y'_\ell(\omega r_0)\Bigr\},\end{aligned} \tag{6.42a}$$

$$\bigl(\Delta\mathfrak{f}_\phi\bigr)_\ell = -2\sum_{m>0}^{\ell}\mathfrak{m}G_{\ell m}Y_{\ell m}(\pi/2,0)\,m\omega\Bigl\{\alpha_\ell(\omega)y_\ell(\omega r_0) + \bigl[\beta_\ell(\omega) - j_\ell(\omega r_0)\bigr]j_\ell(\omega r_0)\Bigr\}, \tag{6.42b}$$

where $\omega = m\Omega$. We observe that the sum over ℓ begins at $\ell = 1$; there is no contribution from $\ell = 0$ because as was first noticed in Sec. VI E, $\Delta P_{\ell m} = 0$ when $\ell = m = 0$. We recall that the sums over m are restricted to values such that $\ell + m$ is even; in this case we find from Eqs. (6.16) and (6.17) that

$$\mathfrak{m}G_{\ell m}Y_{\ell m}(\pi/2,0) = \frac{\mathfrak{m}^2}{\gamma}(2\ell+1)\frac{(\ell-m-1)!!(\ell+m-1)!!}{(\ell-m)!!(\ell+m)!!}. \tag{6.43}$$

The amplitudes $\alpha_\ell(\omega)$ and $\beta_\ell(\omega)$ must be determined numerically by integrating the differential equations that govern the perturbations of the fluid configuration; the shooting method to achieve this was described in Sec. VI C. On the other hand, $Z_\ell - 1$ was obtained analytically in Sec. VI D, and its expression is displayed in Eq. (6.27).

The complete self-force is constructed by combining Eqs. (6.35), (6.37), (6.41), (6.42) and performing the mode sums. An outcome of this computation is that $\dot{\mathfrak{m}} = 0$ — the particle's mass is actually constant when the particle moves on a circular orbit. Our results for the self-force were already displayed in Fig. 2, and we provide additional details in a number of additional figures. In all of them, the compactness of the fluid body is fixed to $\chi = 0.3$. In Fig. 8 we examine the contributions to $\Delta\mathfrak{f}_r$ and $\Delta\mathfrak{f}_\phi$ coming from the lowest multipole orders ℓ in the mode sum, for selected values of r_0. We see that when r_0 is small, the convergence of the mode sum for $\Delta\mathfrak{f}_r$ is slowed down by the resonant features, which can produce abnormally large contributions for selected values of ℓ. We see also that the convergence of the mode sum for $\Delta\mathfrak{f}_\phi$ is considerably faster, and much less affected by the resonant features. In Fig. 9, we display $\mathfrak{f}_r$ and $\mathfrak{f}_\phi$ in small intervals of r_0, and associate each resonant feature with a specific quasinormal mode. We see that the broad resonance observed in Sec. I is associated with the $\ell = 2$ f-mode of the fluid-gravity system, and that the resonance is triggered when $m = 2$, so that $2\Omega = \mathrm{Re}(\omega)$. Finally, note that only resonances with low-ℓ quasinormal modes have been clearly identified in the figures. In fact, as ℓ increases, the modes become longer lived and the resonances get accordingly narrower. To produce Figs. 2 and 9 we sampled more densely the regions where resonances with the computed low-multipole quasinormal modes were expected to arise, and many of the features displayed in these figures could only be identified through this more refined search.

G. Orbital evolution

The self-force computed in the preceding section drives an evolution of the circular orbit: the orbital radius r_0 will slowly decrease because of the dissipative action of the force, and the orbital frequency Ω will also change because of both dissipative and conservative effects. In this subsection we derive and integrate the equations that govern this orbital evolution, exploiting a two-time expansion initially formulated by Pound [38].

We write the orbital equation as

$$\frac{Dv^\alpha}{ds} = \big(\eta^{\alpha\beta} + v^\alpha v^\beta\big)\nabla_\beta\Phi + F^\alpha, \tag{6.44}$$

in which $v^\alpha = dz^\alpha/ds$ is the four-velocity, s is proper time, $\Phi = M/r$ is the background gravitational potential, and $F^\alpha := \mathfrak{m}^{-1}\mathfrak{f}^\alpha$ is the self-force per unit mass. For our purposes it is convenient to adopt the coordinate time t as orbital parameter (instead of proper time s), and in this notation the orbital equation becomes

$$0 = Z^\alpha := \ddot{z}^\alpha + \Gamma^\alpha_{\beta\gamma}\dot{z}^\beta\dot{z}^\gamma + \frac{\dot{\gamma}}{\gamma}\dot{z}^\alpha - \frac{1}{\gamma^2}\Big[\big(g^{\alpha\beta} + \gamma^2\dot{z}^\alpha\dot{z}^\beta\big)\nabla_\beta\Phi + F^\alpha\Big], \tag{6.45}$$

where an overdot now indicates differentiation with respect to t, and $\gamma := dt/ds$ is given by

$$\frac{1}{\gamma^2} = -\eta_{\alpha\beta}\dot{z}^\alpha\dot{z}^\beta. \tag{6.46}$$

We assume that the particle follows a circular orbit with slowly-changing orbital parameters r_0 and Ω. To express this mathematically we introduce a slow-time variable $\bar{t} := \epsilon t$, where $\epsilon \ll 1$, and write

$$r_0 = r_0(\bar{t}), \qquad \Omega = \Omega(\bar{t}). \tag{6.47}$$

The orbital phase ϕ is then obtained by integrating the orbital frequency with respect to (fast) time:

$$\phi = \int \Omega(\bar{t})\, dt = \frac{1}{\epsilon}\int \Omega(\bar{t})\, d\bar{t}. \tag{6.48}$$

With this we find that the vector tangent to the orbit can be expressed as

$$\dot{z}^\alpha = \big(1, \epsilon r_0'(\bar{t}), 0, \Omega(\bar{t})\big), \tag{6.49}$$

in which a prime indicates differentiation with respect to $\bar{t}$. We also have

$$\ddot{z}^\alpha = \big(0, O(\epsilon^2), 0, \epsilon\Omega'(\bar{t})\big). \tag{6.50}$$

With these ingredients we have that $\gamma^{-2} = 1 - r_0^2\Omega^2 + O(\epsilon^2)$, $\dot{\gamma}/\gamma = \epsilon\gamma^2(r_0\Omega^2 r_0' + r_0^2\Omega\Omega')$, and we further expand Ω and F^α in powers of ϵ:

$$\Omega(\bar{t}) = \Omega_0(\bar{t}) + \epsilon\Omega_1(\bar{t}) + O(\epsilon^2), \qquad F^\alpha = \epsilon F_1^\alpha\big(r_0(\bar{t})\big) + O(\epsilon^2). \tag{6.51}$$

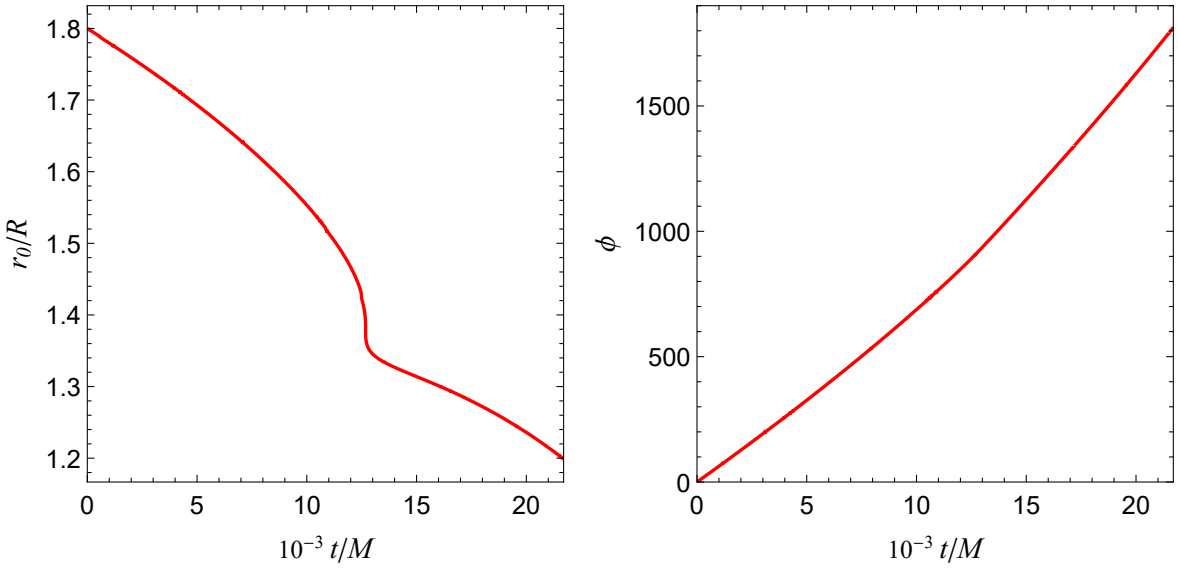

FIG. 10. Plot of the orbital radius r_0/R and the orbital phase ϕ as functions of t/M. The calculations were performed with $\mathfrak{m}/M = 0.01$.

The second equation incorporates an assumption that to leading order in ϵ, the self-force depends only on the orbital radius r_0.

The foregoing relations can all be inserted into the orbital equations $Z^\alpha = 0$, which are then expanded in powers of ϵ. At order ϵ^0, $Z^r = 0$ produces

$$\Omega_0^2 = \frac{M/r_0^3}{1 + M/r_0}, \tag{6.52}$$

the same expression as in Eq. (6.12). At order ϵ, $Z^r = 0$ gives instead

$$\Omega_1 = -\frac{1}{2}(r_0/M)^{1/2}(1 + M/r_0)^{-3/2} F_{1\,r}, \tag{6.53}$$

while $Z^\phi = 0$ yields

$$r_0' = 2(r_0/M)^{1/2}(1 + M/r_0)^{-1/2}(1 + 2M/r_0)^{-1} F_{1\,\phi} + O(\epsilon). \tag{6.54}$$

These equations provide a complete account of the orbital evolution. Reverting to the original notation, we have that

$$\dot{r}_0 = 2(r_0/M)^{1/2}(1 + M/r_0)^{-1/2}(1 + 2M/r_0)^{-1} F_\phi(r_0) + O(\epsilon^2), \tag{6.55a}$$

$$\Omega = \sqrt{\frac{M/r_0^3}{1 + M/r_0}} - \frac{1}{2}(r_0/M)^{1/2}(1 + M/r_0)^{-3/2} F_r(r_0) + O(\epsilon^2), \tag{6.55b}$$

$$\phi = \int \frac{\Omega}{\dot{r}_0}\, dr_0. \tag{6.55c}$$

The equations reveal that $F_\phi := \mathfrak{m}^{-1}\mathfrak{f}_\phi$, the dissipative component of the self-force, determines the evolution of the orbital radius r_0, and therefore the first term in the expression for the angular velocity Ω. They show also that $F_r := \mathfrak{m}^{-1}\mathfrak{f}_r$, the conservative component of the self-force, produces an additional shift in the angular velocity.

We next insert the self-force data obtained previously into these equations, and integrate them numerically to obtain $r_0(t)$, $\Omega(t)$, and $\phi(t)$. For concreteness, we set the mass of the particle to be $\mathfrak{m} = 0.01M$, and compute its evolution from an initial orbit with $r_0 = 1.80$ to a final orbit with $r_0 = 1.20$. Note that a rescaling of the mass would result in a

corresponding rescaling of the inspiral time scale, and would also affect the shift $\Delta\Omega := \Omega - \Omega_0$ of the angular frequency relative to the purely dissipative value. The most revealing information regarding both dissipative and conservative aspects of the orbital evolution is provided by $\Omega(t)$, which was already displayed in Fig. 3 and discussed in Sec. I. In Fig. 10 we also provide plots of $r_0(t)$ and $\phi(t)$. Because $r_0(t)$ is calculated entirely from the dissipative component of the self-force, it is relatively featureless compared with $\Omega(t)$; an exception is the rapid decrease when $t/M \simeq 12,680$, which is caused by the broad resonance near $r_0/R \simeq 1.38$. The orbital phase is also relatively featureless, in spite of the large excursions of the angular velocity produced by the conservative component to the self-force.

ACKNOWLEDGMENTS

One of us (EP) is beholden to the Canadian Institute of Theoretical Astrophysics for its warm hospitality during a research leave from the University of Guelph. This work was supported by the Natural Sciences and Engineering Research Council of Canada, the Conselho Nacional de Desenvolvimento Científico e Tecnológico (CNPq), and the JSPS Postdoctoral Fellowships for Research Abroad.

[1] P. Amaro Seoane et al., *The Gravitational Universe*, arXiv:1305.5720.
[2] S. Kawamura et al., *The Japanese space gravitational wave antenna: DECIGO*, Class. Quantum Grav. **28**, 094011 (2011).
[3] Y. Mino, M. Sasaki, and T. Tanaka, *Gravitational radiation reaction to a particle motion*, Phys. Rev. D **55**, 3457 (1997), arXiv:gr-qc/9606018.
[4] T. C. Quinn and R. M. Wald, *Axiomatic approach to electromagnetic and gravitational radiation reaction of particles in curved spacetime*, Phys. Rev. D **56**, 3381 (1997), arXiv:gr-qc/9610053.
[5] S. E. Gralla and R. M. Wald, *A rigorous derivation of gravitational self-force*, Class. Quantum Grav. **25**, 205009 (2008), arXiv:0806.3293.
[6] A. Pound, *Self-consistent gravitational self-force*, Phys. Rev. D **81**, 024023 (2010), arXiv:0907.5197.
[7] A. Pound, *Singular perturbation techniques in the gravitational self-force problem*, Phys. Rev. D **81**, 124009 (2010), arXiv:1003.3954.
[8] N. Warburton, S. Akcay, L. Barack, J. R. Gair, and N. Sago, *Evolution of inspiral orbits around a Schwarzschild black hole*, Phys. Rev. D **85**, 061501 (2012), arXiv:1111.6908.
[9] T. Osburn, N. Warburton, and C. R. Evans, *Highly eccentric inspirals into a black hole* (2015), arXiv:1511.01498.
[10] S. Isoyama, L. Barack, S. R. Dolan, A. Le Tiec, H. Nakano, A. G. Shah, T. Tanaka, and N. Warburton, *Gravitational self-force correction to the innermost stable circular equatorial orbit of a Kerr black hole*, Phys. Rev. Lett. **113**, 161101 (2014), arXiv:1404.6133.
[11] T. Jacobson and T. P. Sotiriou, *Overspinning a black hole with a test body*, Phys. Rev. Lett. **103**, 141101 (2009), arXiv:0907.4146.
[12] E. Barausse, V. Cardoso, and G. Khanna, *Test bodies and naked singularities: Is the self-force the cosmic censor?*, Phys. Rev. Lett. **105**, 261102 (2010), arXiv:1008.5159.
[13] M. Colleoni and L. Barack, *Overspinning a Kerr black hole: The effect of the self-force*, Phys. Rev. D **91**, 104024 (2015), arXiv:1501.07330.
[14] M. Colleoni, L. Barack, A. G. Shah, and M. van de Meent, *Self-force as a cosmic censor in the Kerr overspinning problem*, Phys. Rev. D **92**, 084044 (2015), arXiv:1508.04031.
[15] S. Detweiler, *Gravitational radiation reaction and second-order perturbation theory*, Phys. Rev. D **85**, 044048 (2012), arXiv:1107.2098.
[16] S. E. Gralla, *Second-order gravitational self-force*, Phys. Rev. D **85**, 124011 (2012), arXiv:1203.3189.
[17] A. Pound, *Second-order gravitational self-force*, Phys. Rev. Lett. **109**, 051101 (2012), arXiv:1201.5089.
[18] A. Pound, *Nonlinear gravitational self-force: Field outside a small body*, Phys. Rev. D **86**, 084019 (2012), arXiv:1206.6538.
[19] A. Pound and J. Miller, *Practical, covariant puncture for second-order self-force calculations*, Phys. Rev. D **89**, 104020 (2014), arXiv:1403.1843.
[20] A. G. Shah, J. L. Friedman, and B. F. Whiting, *Finding high-order analytic post-Newtonian parameters from a high-precision numerical self-force calculation*, Phys. Rev. D **89**, 064042 (2014), arXiv:1312.1952.
[21] N. K. Johnson-McDaniel, A. G. Shah, and B. F. Whiting, *Experimental mathematics meets gravitational self-force*, Phys. Rev. D **92**, 044007 (2015), arXiv:1503.02638.
[22] S. Akcay, A. Le Tiec, L. Barack, N. Sago, and N. Warburton, *Comparison between self-force and post-Newtonian dynamics: Beyond circular orbits*, Phys. Rev. D **91**, 124014 (2015), arXiv:1503.01374.
[23] A. Le Tiec, A. Buonanno, A. H. Mroué, H. P. Pfeiffer, D. A. Hemberger, G. Lovelace, L. E. Kidder, M. A. Scheel, B. Szilágyi, N. W. Taylor, and S. A. Teukolsky, *Periastron advance in spinning black hole binaries: Gravitational self-force from numerical relativity*, Phys. Rev. D **88**, 124027 (2013), arXiv:1309.0541.
[24] L. Barack, *Gravitational self force in extreme mass-ratio inspirals*, Class. Quantum Grav. **26**, 213001 (2009), arXiv:0908.1664.

[25] E. Poisson, A. Pound, and I. Vega, *The motion of point particles in curved spacetime*, Living Rev. Rel. **14**, 7 (2011), arXiv:1102.0529.

[26] P. Zimmerman, I. Vega, E. Poisson, and R. Haas, *Self-force as a cosmic censor*, Phys. Rev. D **87**, 041501 (2013), arXiv:1211.3889.

[27] V. Hubeny, *Overcharging a black hole and cosmic censorship* , Phys. Rev. D **59**, 064013 (1999).

[28] P. Zimmerman and E. Poisson, *Gravitational self-force in nonvacuum spacetimes*, Phys. Rev. D **90**, 084030 (2014), arXiv:1406.5111.

[29] P. Zimmerman, *Gravitational self-force in nonvacuum spacetimes: An effective field theory derivation*, Phys. Rev. D **92**, 064040 (2015), arXiv:1505.03915.

[30] T. M. Linz, J. L. Friedman, and A. G. Wiseman, *Combined gravitational and electromagnetic self-force on charged particles in electrovac spacetimes*, Phys. Rev. D **90**, 084031 (2014), arXiv:1406.5112.

[31] P. Zimmerman, *Gravitational self-force in scalar-tensor gravity*, Phys. Rev. D **92**, 064051 (2015), arXiv:1507.04076.

[32] Y. Kojima, *Stellar resonant oscillations coupled to gravitational waves*, Prog. Theor. Phys. **77**, 297 (1987).

[33] L. Gualtieri, E. Berti, J. A. Pons, G. Miniutti, and V. Ferrari, *Gravitational signals emitted by a point mass orbiting a neutron star: A perturbative approach*, Phys. Rev. D **64**, 104007 (2001), arXiv:gr-qc/0107046.

[34] J. A. Pons, E. Berti, L. Gualtieri, G. Miniutti, and V. Ferrari, *Gravitational signals emitted by a point mass orbiting a neutron star: Effects of stellar structure*, Phys. Rev. D **65**, 104021 (2002), arXiv:gr-qc/0111104.

[35] D. Lai, *Resonant oscillations and tidal heating in coalescing binary neutron stars*, Mon. Not. Roy. Astron. Soc. **270**, 611 (1994).

[36] W. C. G. Ho and D. Lai, *Resonant tidal excitations of rotating neutron stars in coalescing binaries*, Mon. Not. Roy. Astron. Soc. **308**, 153 (1999), arXiv:9812116.

[37] E. Poisson and C. M. Will, *Gravity: Newtonian, Post-Newtonian, Relativistic* (Cambridge University Press, Cambridge, England, 2014).

[38] A. Pound, *Second-order perturbation theory: problems on large scales* (2015), arXiv:1510.05172.

[39] N. Deruelle, *Nordström's scalar theory of gravity and the equivalence principle*, Gen. Relativ. and Grav. **43**, 3337 (2011), arXiv:1104.4608.

[40] T. Damour and G. Esposito-Farse, *Tensor-multi-scalar theories of gravitation*, Class. Quantum Grav. **9**, 2093 (1992).

[41] J. L. Friedman and N. Stergioulas, *Rotating relativistic stars* (Cambridge University Press, Cambridge, 2013).

[42] W. H. Press, S. A. Teukolsky, W. T. Vetterling, and B. P. Flannery, *Numerical Recipes in C++: The Art of Scientific Computing, Second Edition* (Cambridge University Press, Cambridge, England, 2002).

[43] T. Drivas and S. Gralla, *Dependence of self-force on central object*, Class. Quantum Grav. **28**, 145025 (2011).